TU Graz
SCIENCE
PASSION
TECHNOLOGY

6G Beyond Communications: **Positioning, Sensing, and Wireless Power Transfer**

Klaus Witrisal, 1-9-2022

Summer School: "Defining 6G", Linköping, SE

Joint work with my research team and alumni:
Erik Leitinger, Thomas Wilding, Benjamin Deutschmann, Alexander Venus, Lukas Wielandner, Andreas Fuchs, Agnes Koller, Mate Toth, Jakob Möderl, Anh Nguyen, Stefan Grebien, Michael Rath, Josef Kulmer, Paul Meissner

Technologies for 6G:

- **BW / frequency** scaling: microwave → mmWave → THz
- **Cell** scaling: small cells → cell-free; coordinated multi point
- **Antenna** scaling / diversity: mMIMO → physically large arrays; distributed mMIMO
- **Channel** control: reconfigurable intelligent surfaces
- Edge cloud: local computing and storage

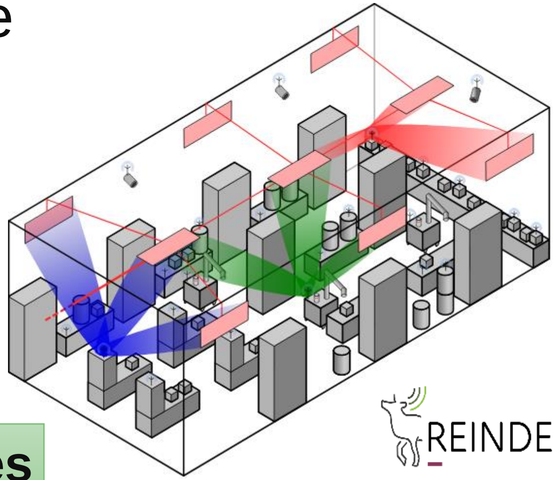

RadioWeaves

REINDEER

RadioWeaves: Features and Use Cases

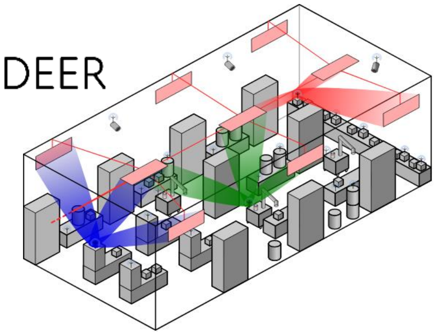

Superior performance:

- Troughput, reliability, latency
- **Energy efficiency**
- **Position accuracy,** reliability

New features:

- **Sensing:** device-free localization
- Mapping; environment awareness
- **Wireless power transfer**

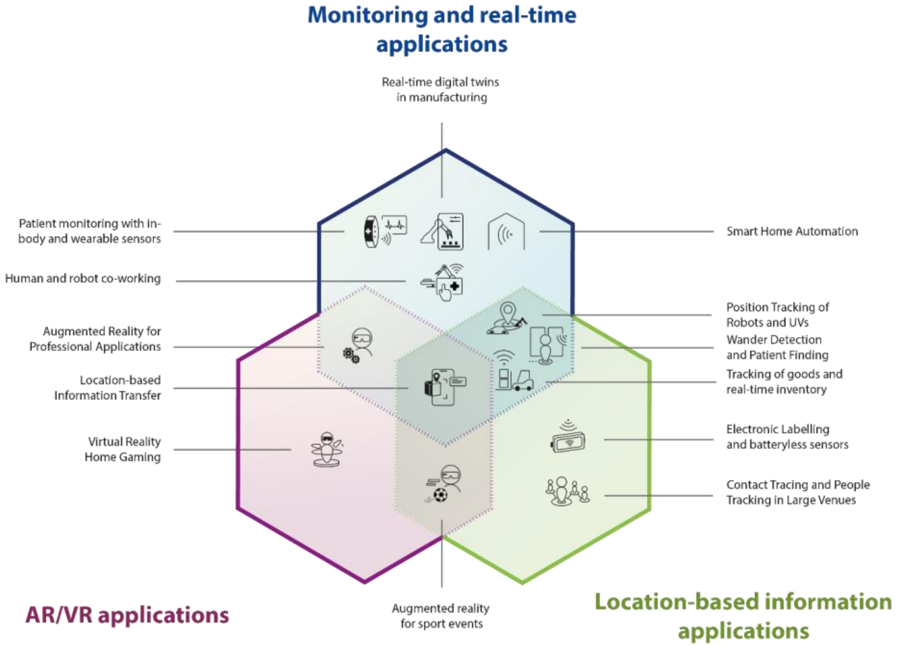

[“Use case-driven specifications and technical requirements and initial channel model”, Project REINDEER, H2020-ICT-52-2020, D1.1, Sept. 2021]

Environment awareness / situational awareness

Awareness of:

- **own** location and pose
- **other** users / agents / nodes
- **environment** (sensing; channel state information)

Benefits for:

- energy efficient resource allocation
- massive deployment
- predictable reliability
- imperceivable latency
- robust position tracking

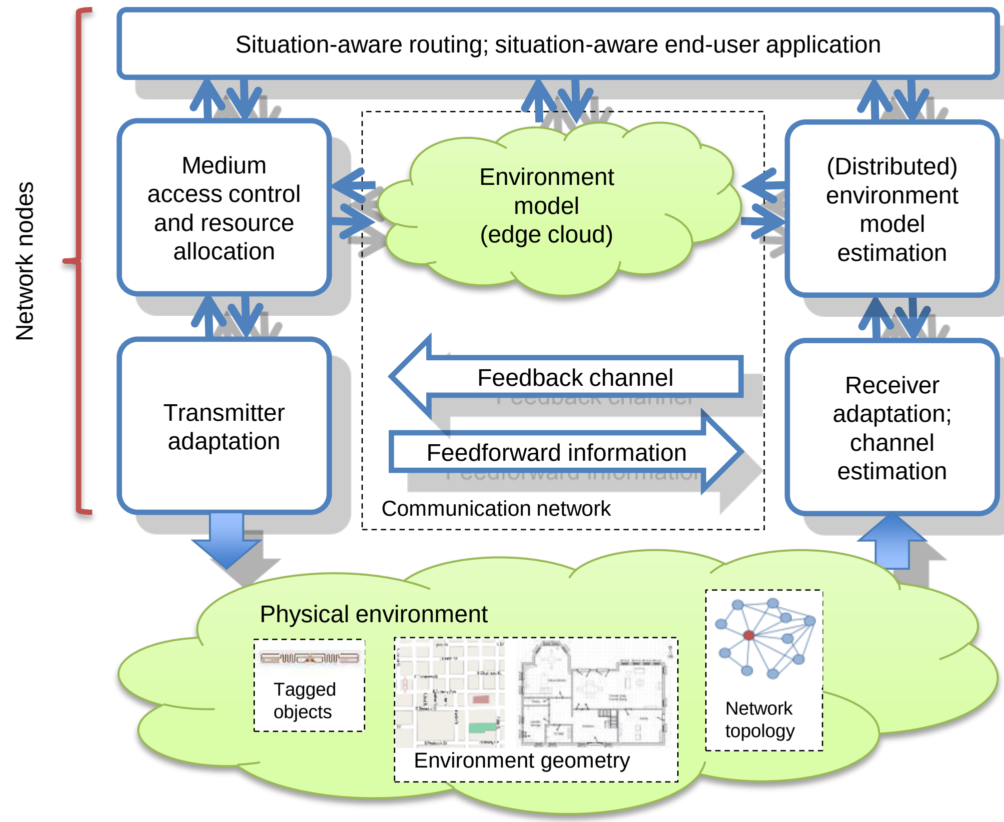

Outline

- Introduction
- **Ranging and positioning in dense multipath**
  - **Bandwidth scaling and MIMO gain**
- Sensing
  - Multipath-assisted indoor positioning
  - Environment modeling
- Wireless Power Transfer
  - With physically large arrays
- Conclusions

An experiment:

transmission of a (UWB) pulse in an indoor environment

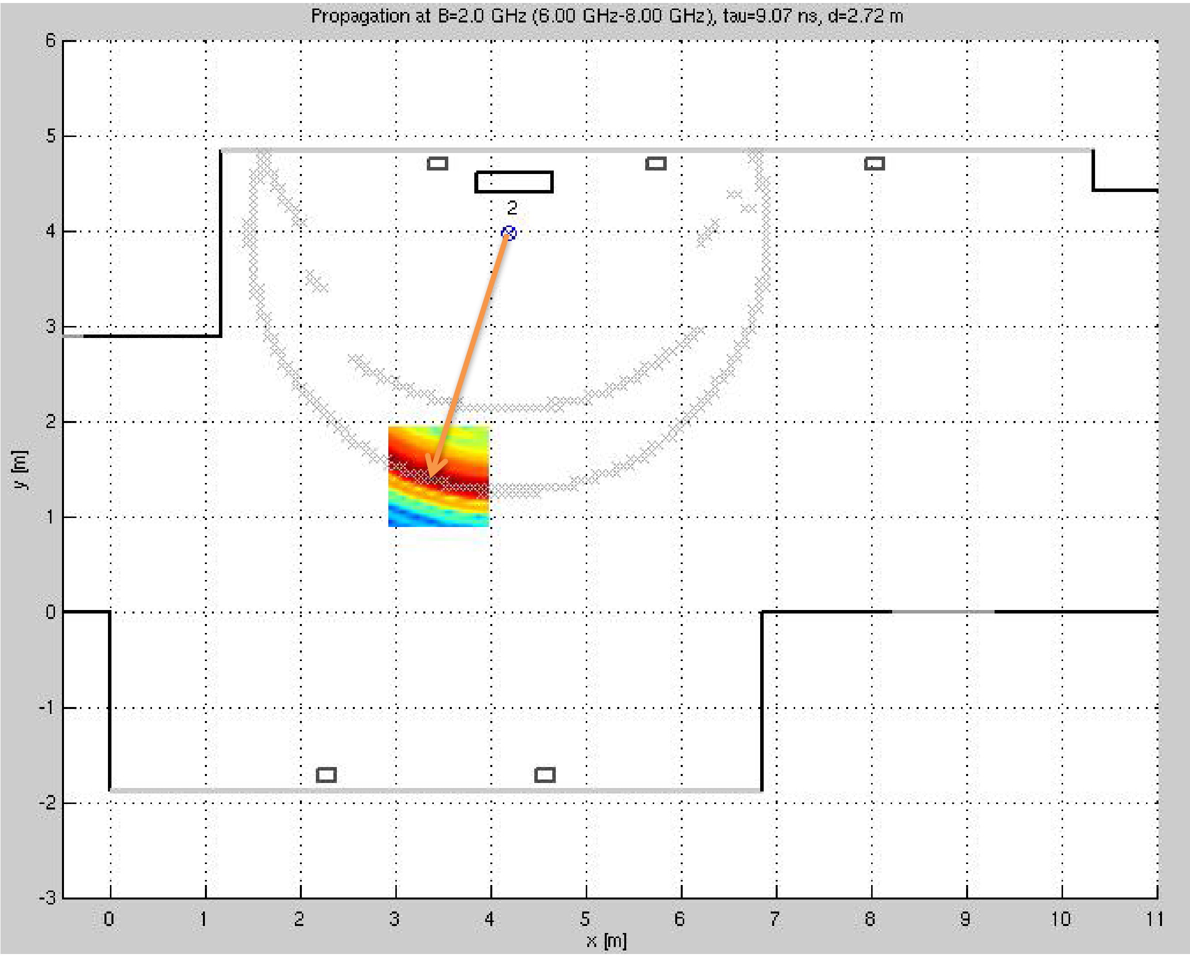

Time-of-flight Ranging

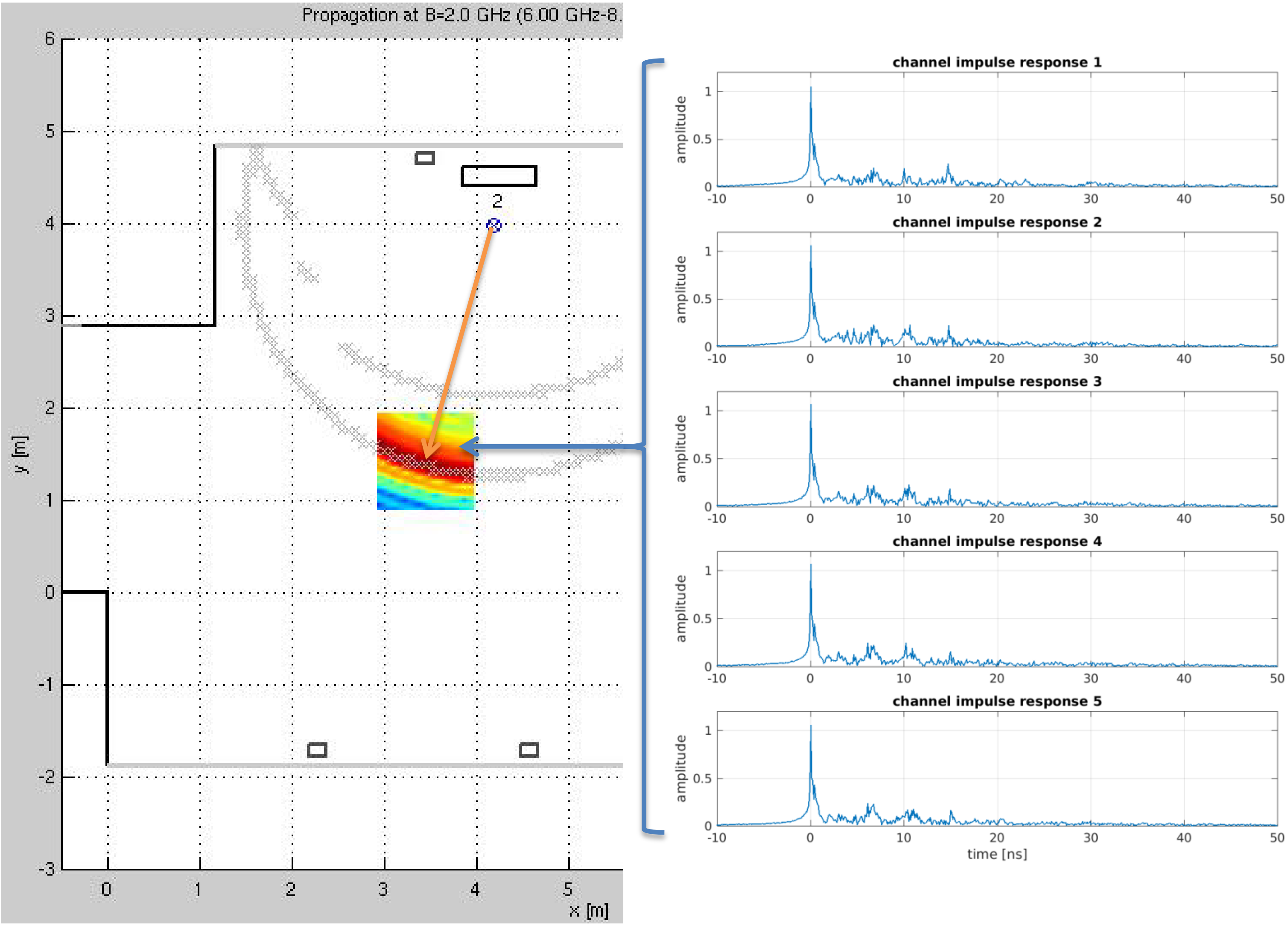

Time-of-flight Ranging:

Problem: Multipath Radio Propagation

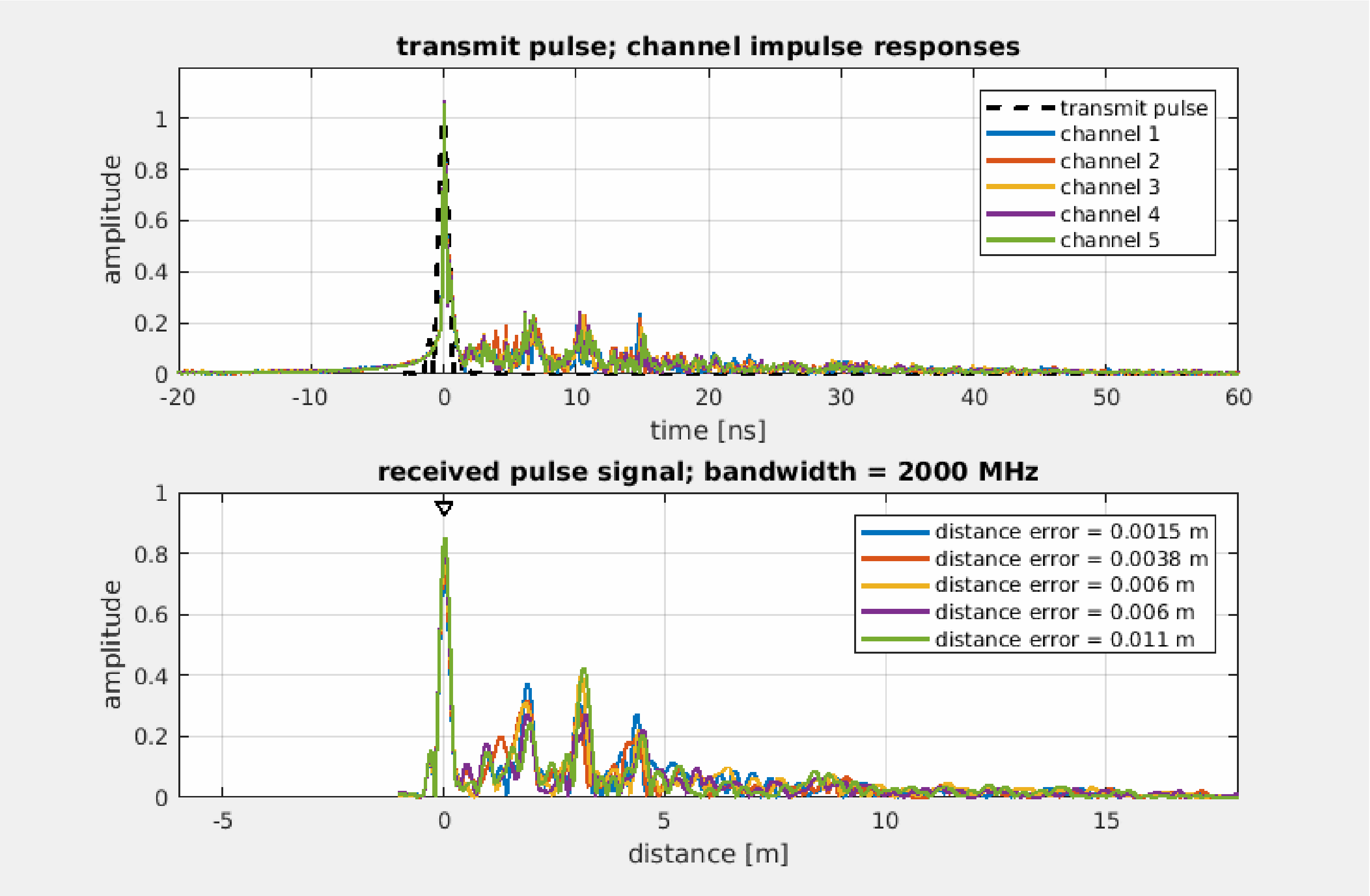

Time-of-flight Ranging:

Problem: Multipath Radio Propagation

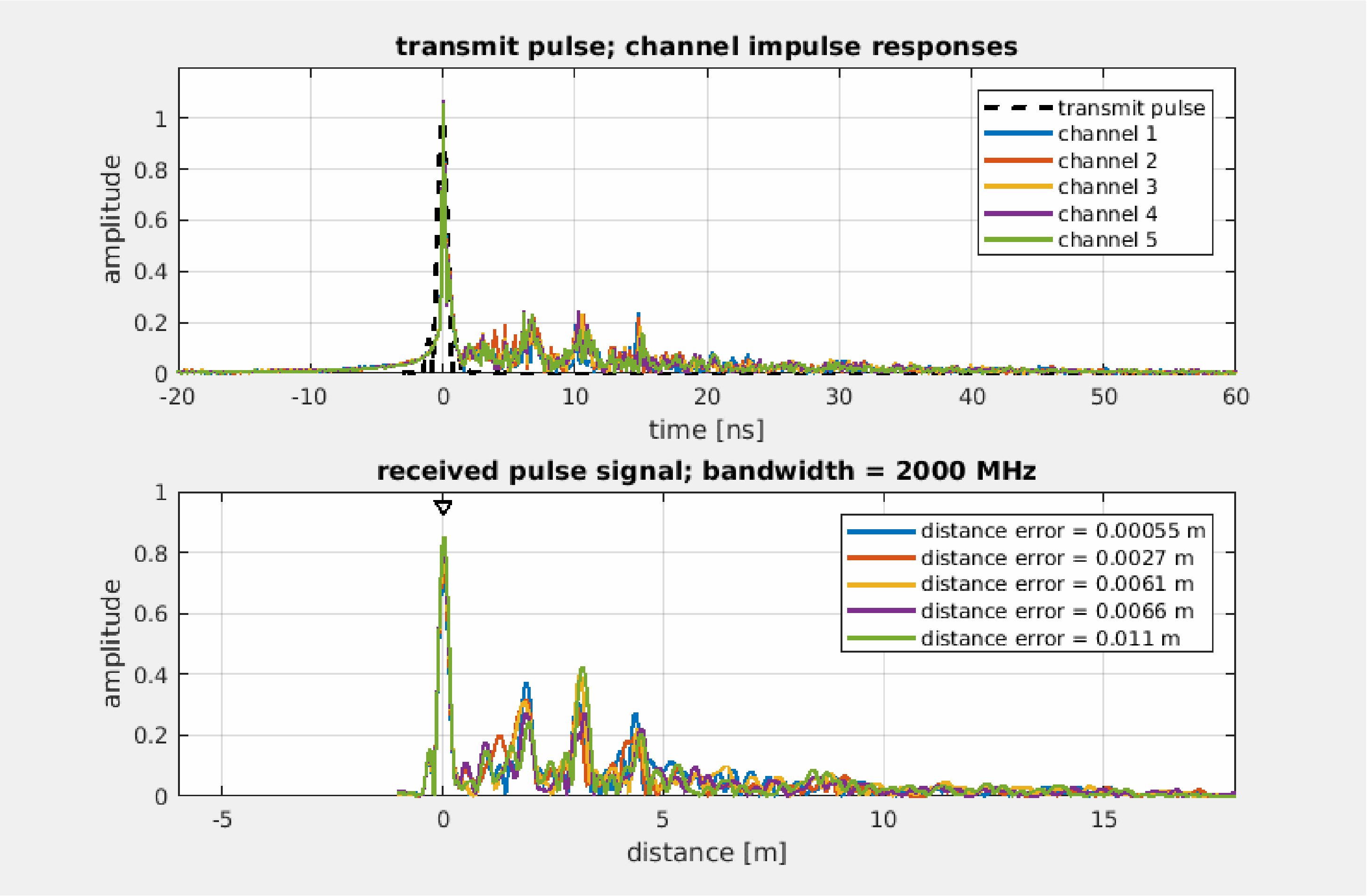

Time-of-flight Ranging:

Problem: Multipath Radio Propagation

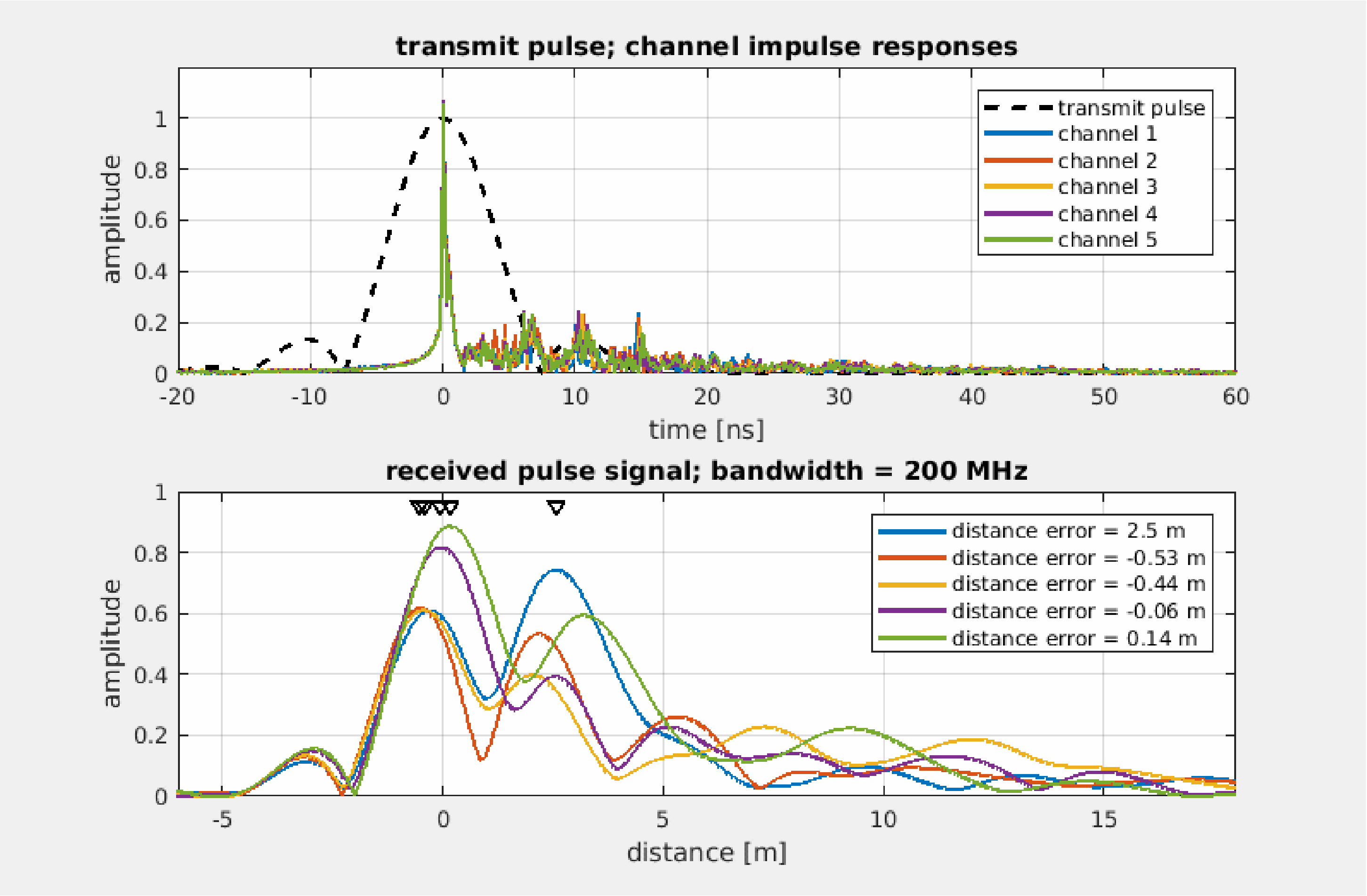

Time-of-flight Ranging:
Problem: Multipath Radio Propagation

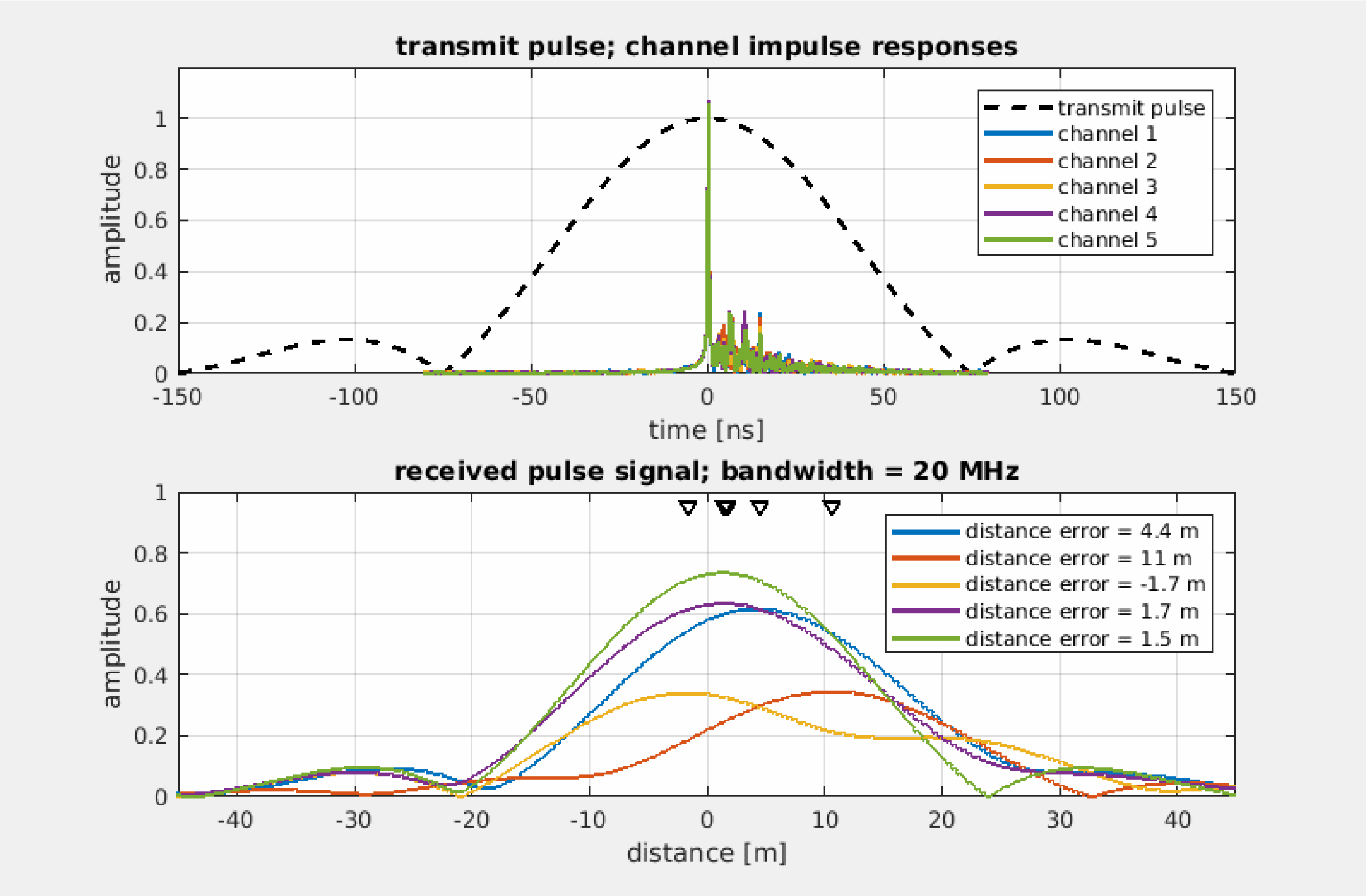

Signal Processing for Robust Ranging (& Pos.)

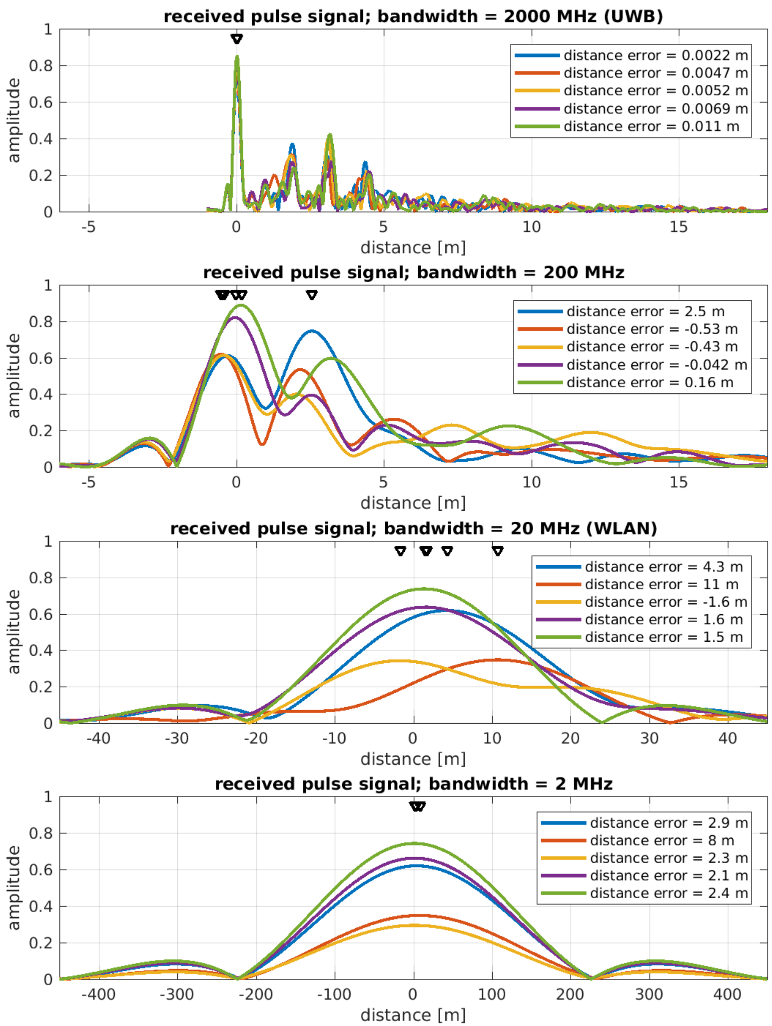

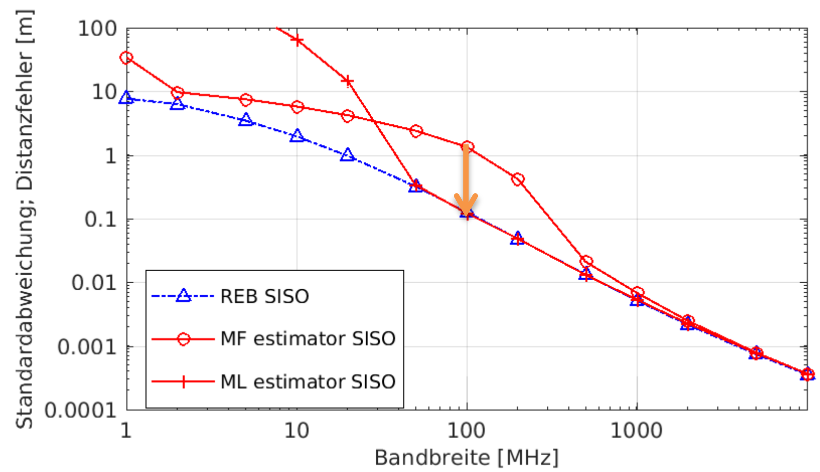

- Experiment
- Modelling
- Performance limits
- Algorithms

Modeling the dense multipath

to derive the theoretical limit (CRLB)

Received signal from anchor *j* located at $\mathbf{p}^{(j)}$: ($s(t)$: TX signal)

$$r^{(j)}(t) = \underbrace{\alpha^{(j)} s(t-\tau^{(j)})}_{\text{useful signal}} + \underbrace{(s * \nu^{(j)})(t)}_{\text{interference}} + \underbrace{w(t)}_{\text{noise}}$$

$$\tau^{(j)} = \frac{1}{c}\|\mathbf{p} - \mathbf{p}^{(j)}\|$$

$$\mathrm{E}\{\nu(\tau)\nu^*(u)\} = S_\nu(\tau)\delta(\tau - u)$$

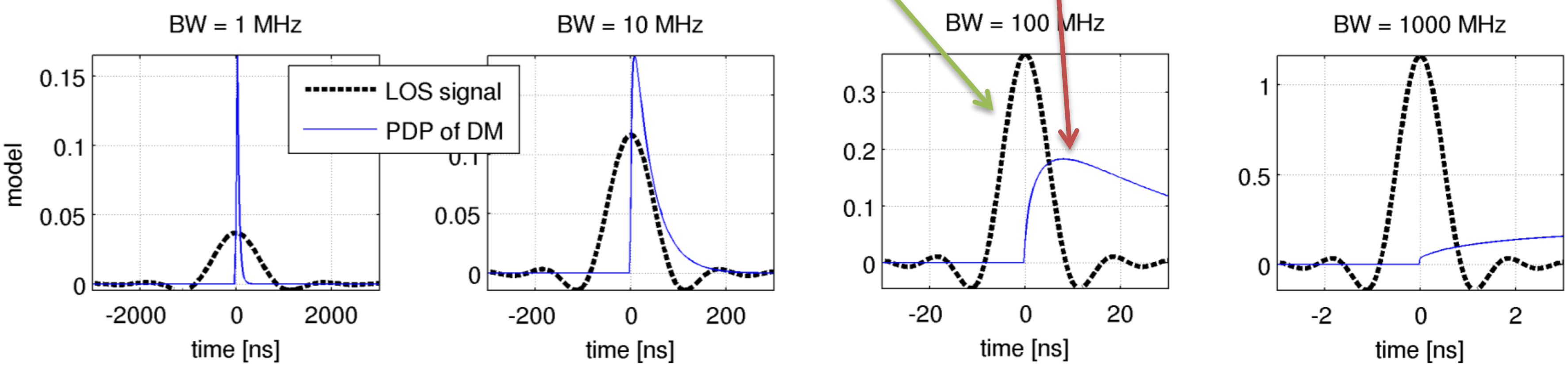

[Witrisal et al. "Bandwidth Scaling and Diversity Gain for Ranging and Positioning in Dense Multipath Channels," IEEE Wireless Commun. Lett., 2016.]

Likelihood function for ranging (in DM)

- **Vector** signal model
  - noise and DM modeled as a Gaussian process

$$\mathbf{r} = \alpha \mathbf{s}(\tau_0) + \boldsymbol{\nu} + \mathbf{w} \qquad \mathbf{C}_\mathrm{n} = \mathbb{E}\{(\boldsymbol{\nu} + \mathbf{w})(\boldsymbol{\nu} + \mathbf{w})^\mathrm{H}\}$$

- **Likelihood** for delay estimation (ranging, ToA)

$$f(\mathbf{r}; \tau, \alpha) \propto \exp\left\{-(\mathbf{r} - \mathbf{s}(\tau)\alpha)^\mathrm{H} \mathbf{C}_\mathrm{n}^{-1} (\mathbf{r} - \mathbf{s}(\tau)\alpha)\right\}$$

- Allows for derivation of:

Cramer-Rao lower bound (CRLB):

$$\mathrm{var}(\hat{\tau}) \geq \frac{1}{-\mathbb{E}\left[\frac{\partial^2 \ln f(\mathbf{r};\tau)}{\partial \tau^2}\right]}$$

Maximum likelihood (ML) estimator:

$$\hat{\tau} = \arg\max_{\tau} f(\mathbf{r}; \tau)$$

ML estimation (in AWGN)

- Maximizing the LHF for model parameters; **AWGN**

$$(\hat{\tau}, \hat{\alpha}) = \arg\max_{\tau,\alpha} \exp\left\{-(\mathbf{r} - \mathbf{s}(\tau)\alpha)^{\mathrm{H}} \mathbf{C}_{\mathrm{n}}^{-1} (\mathbf{r} - \mathbf{s}(\tau)\alpha)\right\}$$
$$= \arg\min_{\tau,\alpha} \|\mathbf{r} - \mathbf{s}(\tau)\alpha\|^2$$

- nuisance parameter α: **projection theorem**

$$\mathbf{s}^{\mathrm{H}}(\tau)(\mathbf{r} - \mathbf{s}(\tau)\hat{\alpha}) = 0 \qquad \hat{\alpha}(\tau) = \frac{\mathbf{s}^{\mathrm{H}}(\tau)\mathbf{r}}{\|\mathbf{s}(\tau)\|^2}$$

- yields

$$\hat{\tau} = \arg\min_{\tau} \|\mathbf{r} - \mathbf{s}(\tau)\hat{\alpha}(\tau)\|^2$$
$$= \arg\max_{\tau} |\hat{\alpha}(\tau)|$$
$$= \arg\max_{\tau} |\mathbf{s}^{\mathrm{H}}(\tau)\mathbf{r}|$$

This is a **matched filter**!

ML estimation in AWGN: **Matched Filter**

- TX and RX signals:

Channel IR

$$s(t) \qquad\qquad r(t) = (s * h)(t) + w(t)$$

- Matched filter:

$$\overleftarrow{s}(t) = s^*(-t)$$

- Yields **filtered channel impulse response:**

$$\hat{\alpha}(\tau) = (s * h * \overleftarrow{s})(\tau) + (w * \overleftarrow{s})(\tau)$$
$$= (h * \rho_s)(\tau) + \tilde{w}(\tau)$$

Signal ACF

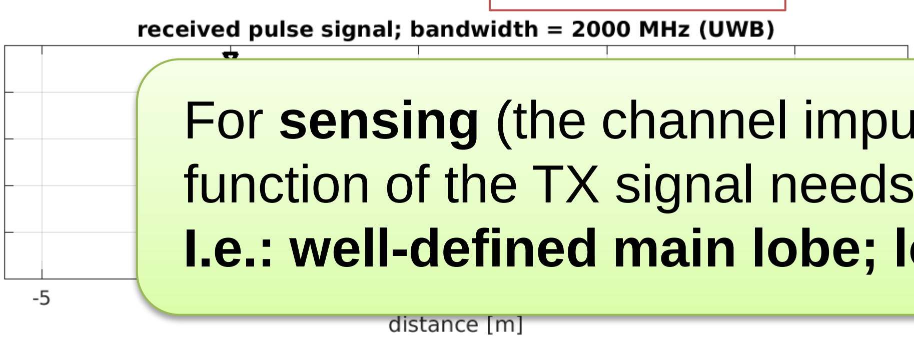

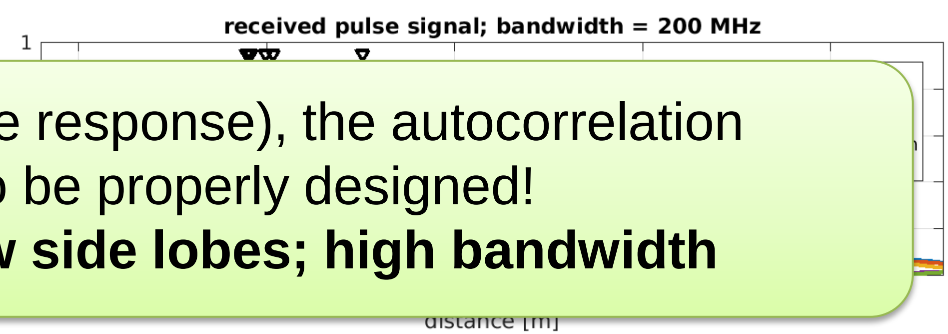

For **sensing** (the channel impulse response), the autocorrelation function of the TX signal needs to be properly designed!
I.e.: well-defined main lobe; low side lobes; high bandwidth

Signal design for ranging in AWGN: OFDM

- TX signal by IFFT $\mathbf{s} = \mathbf{F}^{-1}\tilde{\mathbf{s}}$
- RX signal after FFT
$$\begin{aligned}\tilde{\mathbf{r}} &= \mathbf{F}\mathbf{H}\mathbf{F}^{-1}\tilde{\mathbf{s}} + \mathbf{F}\mathbf{w} \\ &= \tilde{\mathbf{H}}\tilde{\mathbf{s}} + \tilde{\mathbf{w}}\end{aligned}$$
  - with **(diagonal!)** channel frequency respose matrix
$$\begin{aligned}\tilde{\mathbf{H}} &= \mathrm{diag}[H(0), H(\Delta_f), H(2\Delta_f), \cdots, H(-\Delta_f)] \\ &= \alpha\, \mathrm{diag}[e^0, e^{-j2\pi\Delta_f\tau_0}, e^{-j4\pi\Delta_f\tau_0}, \cdots, e^{j2\pi\Delta_f\tau_0}]\end{aligned}$$
  - where second line is for **delay channel**
$$h(t) = \alpha\delta(t-\tau_0)$$
- The ML estimator: project $\tilde{\boldsymbol{r}}$ onto
$$\tilde{\mathbf{s}}(\tau) = [e^0, e^{-j2\pi\Delta_f\tau}, e^{-j4\pi\Delta_f\tau}, \cdots, e^{j2\pi\Delta_f\tau}]^{\mathrm{T}}$$
  - this is **Fourier transform** of **rectangular pulse!**
  - can use insight in **windowing** to optimize pulse design

Range ambiguity function

for ToA estimation with an OFDM pilot

- OFDM signal: 48 SCs at 0.3125 kHz spacing (BW =16 MHz)
- Channel: one tap at 0.5 μs, α = 10; **second** at 0.75 μs, α = 1
- Window: Rectangular, Hamming

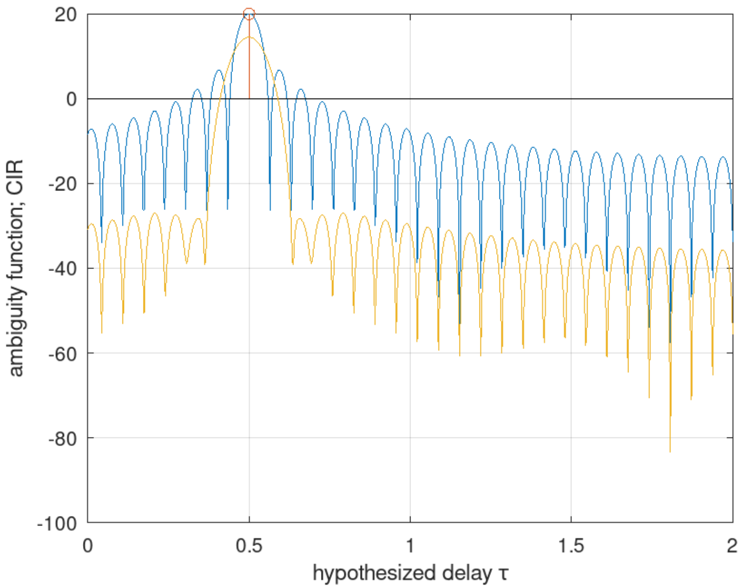

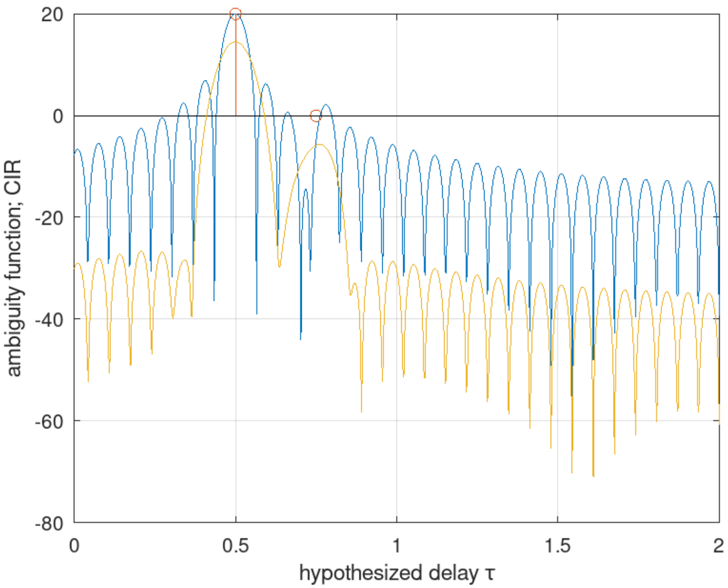

Likelihood function for ranging (in DM)

- **Vector** signal model
  - noise and DM modeled as a Gaussian process

$$\mathbf{r} = \alpha \mathbf{s}(\tau_0) + \boldsymbol{\nu} + \mathbf{w} \qquad \mathbf{C}_\mathrm{n} = \mathbb{E}\{(\boldsymbol{\nu} + \mathbf{w})(\boldsymbol{\nu} + \mathbf{w})^\mathrm{H}\}$$

- **Likelihood** for delay estimation (ranging, ToA)

$$f(\mathbf{r}; \tau, \alpha) \propto \exp\left\{-(\mathbf{r} - \mathbf{s}(\tau)\alpha)^\mathrm{H} \mathbf{C}_\mathrm{n}^{-1} (\mathbf{r} - \mathbf{s}(\tau)\alpha)\right\}$$

- Allows for derivation of:

Cramer-Rao lower bound (CRLB):

$$\mathrm{var}(\hat{\tau}) \geq \frac{1}{-\mathbb{E}\left[\frac{\partial^2 \ln f(\mathbf{r};\tau)}{\partial \tau^2}\right]}$$

Maximum likelihood (ML) estimator:

$$\hat{\tau} = \arg\max_{\tau} f(\mathbf{r}; \tau)$$

CRLB for ranging in DM: **derivation**

- CRLB for parameter vector $\boldsymbol{\psi} = [\tau, \Re\alpha, \Im\alpha]^{\mathrm{T}}$

$$\mathrm{var}(\hat{\tau}) \geq [\boldsymbol{\mathcal{I}}_{\boldsymbol{\psi}}^{-1}]_{1,1} \qquad \boldsymbol{\mathcal{I}}_{\boldsymbol{\psi}} = \mathbb{E}_{\mathbf{r}|\boldsymbol{\psi}}\left\{\left[\frac{\partial}{\partial \boldsymbol{\psi}} \ln f(\mathbf{r}|\boldsymbol{\psi})\right]\left[\frac{\partial}{\partial \boldsymbol{\psi}} \ln f(\mathbf{r}|\boldsymbol{\psi})\right]^{\mathrm{T}}\right\}$$

  - elements of the **Fisher information matrix:**

$$[\boldsymbol{\mathcal{I}}_{\boldsymbol{\psi}}]_{1,1} = 2|\alpha|^2 \dot{\mathbf{s}}(\tau)^{\mathrm{H}} \mathbf{C}_{\mathrm{n}}^{-1} \dot{\mathbf{s}}(\tau) + \mathrm{tr}\left[\mathbf{C}_{\mathrm{n}}^{-1} \frac{\partial \mathbf{C}_{\mathrm{n}}}{\partial \tau} \mathbf{C}_{\mathrm{n}}^{-1} \frac{\partial \mathbf{C}_{\mathrm{n}}}{\partial \tau}\right]$$

$$[\boldsymbol{\mathcal{I}}_{\boldsymbol{\psi}}]_{1,2} = [\boldsymbol{\mathcal{I}}_{\boldsymbol{\psi}}]_{2,1} = 2\Re\{\alpha\} \mathbf{s}(\tau)^{\mathrm{H}} \mathbf{C}_{\mathrm{n}}^{-1} \dot{\mathbf{s}}(\tau)$$

$$[\boldsymbol{\mathcal{I}}_{\boldsymbol{\psi}}]_{1,3} = [\boldsymbol{\mathcal{I}}_{\boldsymbol{\psi}}]_{3,1} = 2\Im\{\alpha\} \mathbf{s}(\tau)^{\mathrm{H}} \mathbf{C}_{\mathrm{n}}^{-1} \dot{\mathbf{s}}(\tau) \qquad \dot{\mathbf{s}}(\tau) = \partial \mathbf{s}(\tau)/\partial \tau$$

$$[\boldsymbol{\mathcal{I}}_{\boldsymbol{\psi}}]_{2,2} = [\boldsymbol{\mathcal{I}}_{\boldsymbol{\psi}}]_{3,3} = 2\mathbf{s}(\tau)^{\mathrm{H}} \mathbf{C}_{\mathrm{n}}^{-1} \mathbf{s}(\tau)$$

$$[\boldsymbol{\mathcal{I}}_{\boldsymbol{\psi}}]_{2,3} = [\boldsymbol{\mathcal{I}}_{\boldsymbol{\psi}}]_{3,2} = 0$$

  - **yields:**

$$\mathcal{I}_{\tau} = 2\frac{|\alpha|^2}{\sigma_{\mathrm{n}}^2} \|\dot{\mathbf{s}}(\tau)\|_{\mathcal{H}}^2 \left(1 - \frac{|\langle \dot{\mathbf{s}}(\tau), \mathbf{s}(\tau)\rangle_{\mathcal{H}}|^2}{\|\dot{\mathbf{s}}(\tau)\|_{\mathcal{H}}^2 \|\mathbf{s}(\tau)\|_{\mathcal{H}}^2}\right) + \mathrm{tr}\,[\bullet]$$

$$\langle \mathbf{x}, \mathbf{y}\rangle_{\mathcal{H}} = \sigma_{\mathrm{n}}^2 \mathbf{y}^{\mathrm{H}} \mathbf{C}_{\mathrm{n}}^{-1} \mathbf{x}$$

$$\|\mathbf{x}\|_{\mathcal{H}}^2 = \langle \mathbf{x}, \mathbf{x}\rangle_{\mathcal{H}}$$

CRLB for ranging (in dense multipath (DM))

AWGN only

$$r_\ell(t) = \alpha_\ell s(t - \tau_\ell) + w(t)$$

CRLB

$$\boxed{\mathrm{var}\{\hat{\tau}\} \geq \left(8\pi^2\beta^2\mathrm{SNR}\right)^{-1}}$$

- mean-squared bandwidth

$$\beta^2 = \int_f f^2 |S(f)|^2 \mathrm{d}f$$

- signal-to-noise ratio

$$\mathrm{SNR} = \frac{E_{\mathrm{LOS}}}{N_0}$$

➢ CRLB scales with **squared bandwidth** and SNR

AWGN + dense multipath

$$r_\ell(t) = \alpha_\ell s(t - \tau_\ell) + \underline{(s * \nu_\ell)(t)} + w(t)$$

CRLB → interference

$$\boxed{\mathrm{var}\{\hat{\tau}\} \geq \left(8\pi^2\beta^2\widetilde{\mathrm{SINR}}\right)^{-1}}$$

- whitening *gain*

$$\beta_{\mathrm{w}}^2 = \beta^2\gamma; \quad \gamma \geq 1$$

- *reduced* SNR due to DM

$$\mathrm{SINR} = \frac{E_{\mathrm{LOS}}}{N_0 + \mathrm{DM}} \leq \mathrm{SNR}$$

- *cost* for nuissance estim.

$$\sin^2(\varphi) \in [0, 1]$$

[Witrisal et al. "Bandwidth Scaling and Diversity Gain for Ranging and Positioning in Dense Multipath Channels," IEEE Wireless Commun. Lett., 2016.]

Ranging error bound and SINR

shows the *bandwidth scaling*

bandwidth

$$\mathrm{var}\{\hat{\tau}\} \geq \left(8\pi^2\beta^2\widetilde{\mathrm{SINR}}\right)^{-1}$$

$$\widetilde{\mathrm{SINR}} = \gamma \mathrm{SINR}\sin^2(\varphi)$$

CRLB
in AWGN

Parameters

- *SNR = 30 dB*
- K_{LOS} = 1 … LOS-to-DM-power

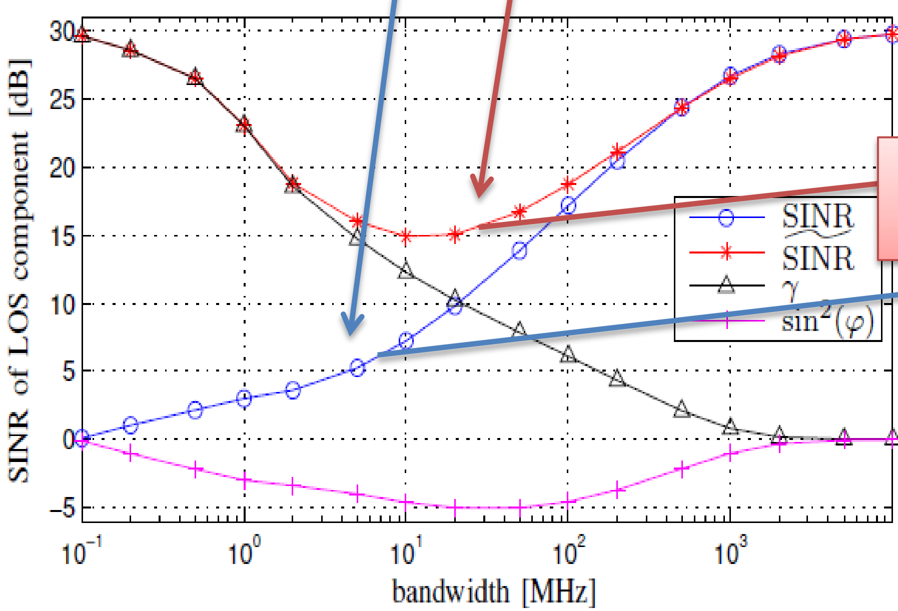

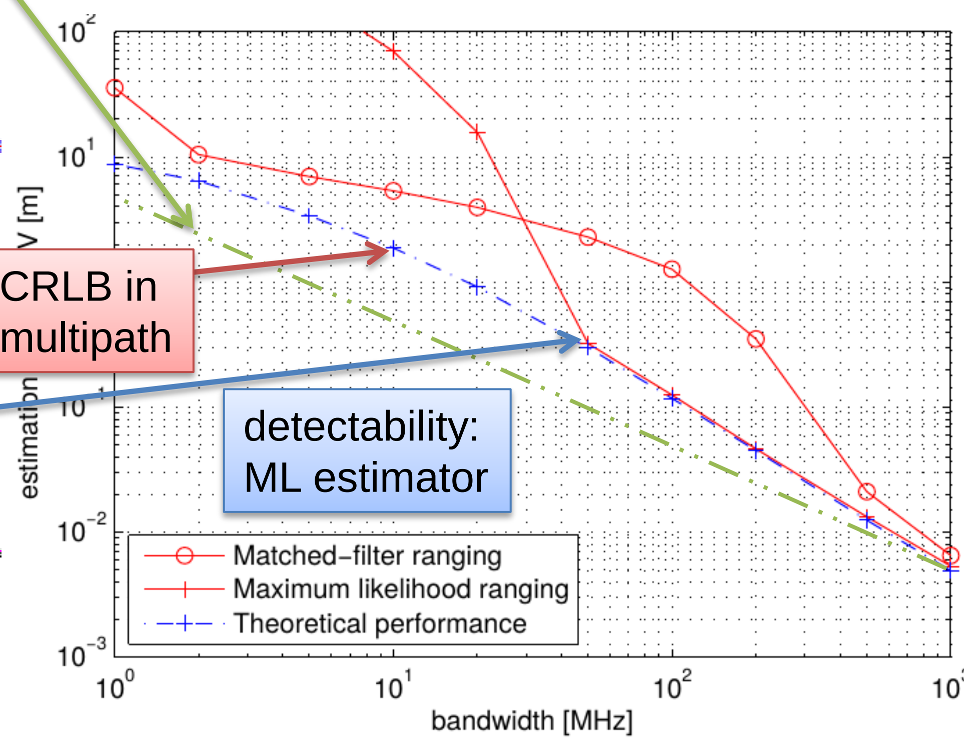

CRLB in
multipath

detectability:
ML estimator

[Witrisal et al. "Bandwidth Scaling and Diversity Gain for Ranging and Positioning in Dense Multipath Channels," IEEE Wireless Commun. Lett., 2016.]

Position error bound

Equivalent Fisher information $\mathbf{J}_{\mathbf{p}}$

Position error variance *(CRLB):*

$$\mathrm{var}\{\hat{\mathbf{p}}\} \geq \mathrm{tr}\{\mathbf{J}_{\mathbf{p}}^{-1}\}$$

- *J independent* measurements:

ranging direction matrix

$$\mathbf{J}_{\mathbf{p}} = \frac{8\pi^2\beta^2}{c^2}\sum_{j=1}^{J}\widetilde{\mathrm{SINR}}^{(j)}\mathbf{J}_{\mathrm{r}}(\phi^{(j)})$$

geometry of nodes

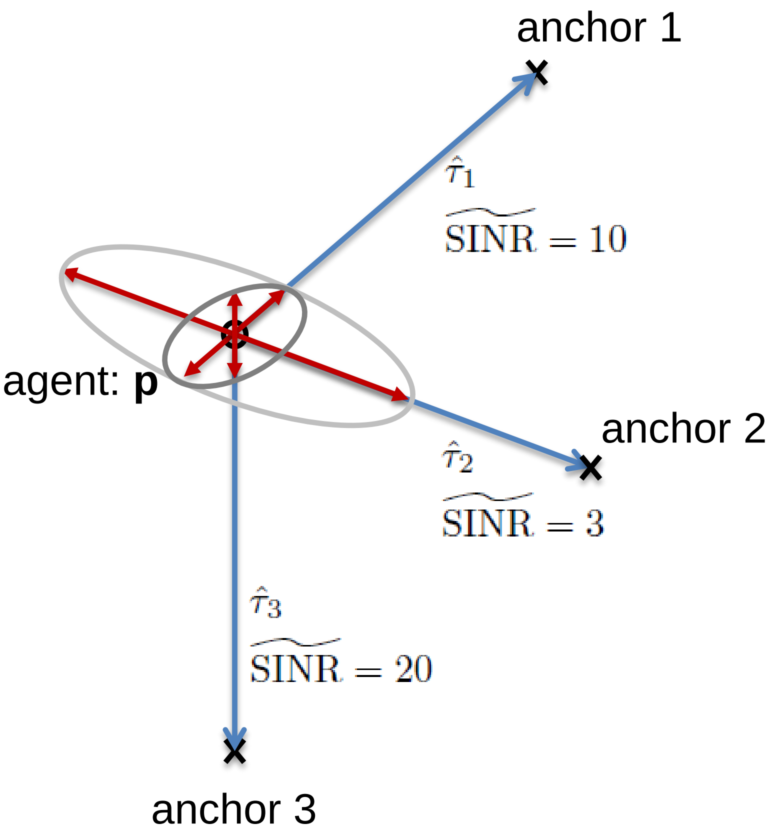

[Y. Shen and M. Win, "Fundamental Limits of Wideband Localization; Part I: A General Framework," IEEE Trans. Inform. Theory, vol. 56, no. 10, pp. 4956-4980, October 2010.]

Diversity (MIMO) **gain**

Fisher information $\mathbf{J_p}$

- *J independent* measurements:

$$\mathbf{J_p} = \frac{8\pi^2\beta^2}{c^2}\sum_{j=1}^{J}\widetilde{\mathrm{SINR}}^{(j)}\mathbf{J_r}(\phi^{(j)})$$

Diversity combining (SIMO, MISO, MIMO):

- approx. equal geometries
- effective SINRs are added up:

$$\mathbf{J_p} = \frac{8\pi^2\beta^2}{c^2}\sum_{\ell=1}^{L}\underbrace{\left[\sum_{j\in\mathcal{N}_\ell}\widetilde{\mathrm{SINR}}^{(j)}\right]}_{\text{SINR gain}}\mathbf{J_r}(\phi_\ell)$$

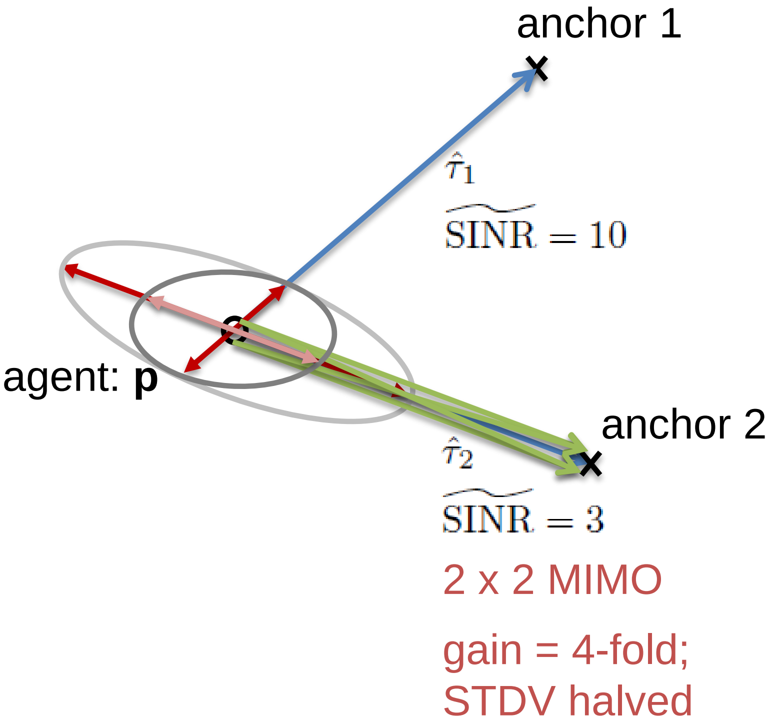

[Witrisal et al. "Bandwidth Scaling and Diversity Gain for Ranging and Positioning in Dense Multipath Channels," IEEE Wireless Commun. Lett., 2016.]

Multi-antenna configurations – *diversity (MIMO) gain for ranging*

- **4 x 4 MIMO** vs. SISO (1 x 1)
  - 16 independent measm.
  - 16-fold SINR (LOS-to-multipath-power-ratio):
- theoretical limit reduced by **factor 4**
- **detection probability** strongly improved

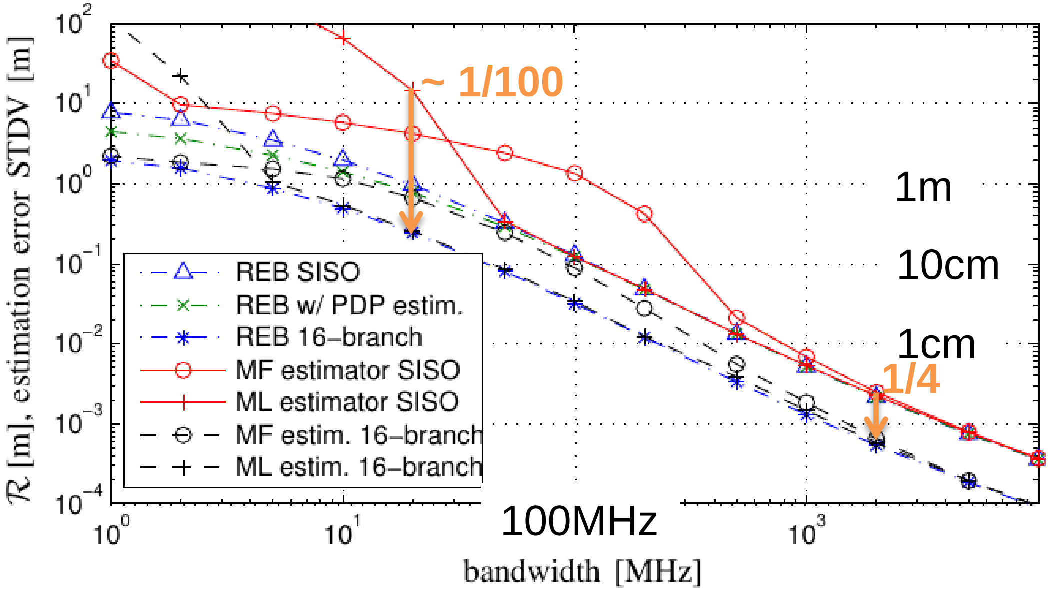

[Witrisal et al. "Bandwidth Scaling and Diversity Gain for Ranging and Positioning in Dense Multipath Channels," IEEE Wireless Commun. Lett., 2016.]

Position error bound and MIMO gain:
applied to multistatic RFID positioning

Three configurations are compared:

1. Each reader has:
   - 1 antenna for TX and RX (1 TRX)
   - yielding **2 range** measurements

2. Each reader has:
   - separated TX/RX antennas
   - yielding **2 range** + **2 bistatic** meas.

3. Each reader has
   - 2 pairs of separated TX/RX ant.
   - yielding **8 independent** range plus **8 independent** bistatic measurem.

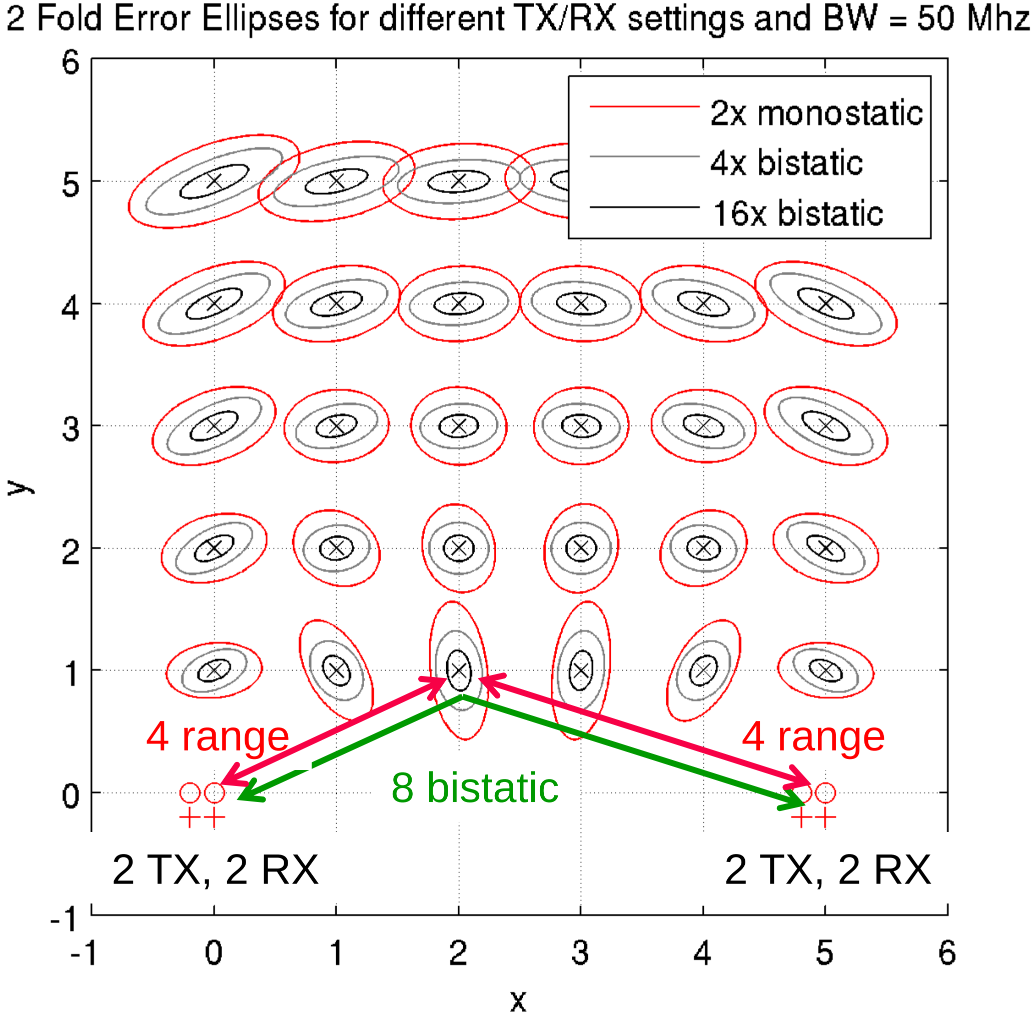

[Hinteregger, Witrisal, et al., "MIMO Gain and Bandwidth Scaling for RFID Positioning in Dense Multipath Channels," in 2016 IEEE Intern. Conf. on RFID, 2016.]

Positioning Performance Bounds

- Multiple anchors; delay and angle information from LOS

$$\boldsymbol{I}(\boldsymbol{p}) \approx \sum_{l=1}^{L} \underbrace{\frac{8\pi^2\,\mathrm{SINR}^{(l)}\,D_\lambda^2(\phi^{(l)})\,M}{(c\tau^{(l)})^2}\boldsymbol{U}_\mathrm{r}^{\perp}(\phi^{(l)})}_{\text{AoA}} + \underbrace{\frac{8\pi^2\beta^2\,\widetilde{\mathrm{SINR}}_\tau^{(l)}\,M}{c^2}\boldsymbol{U}_\mathrm{r}(\phi^{(l)})}_{\text{ToA}}$$

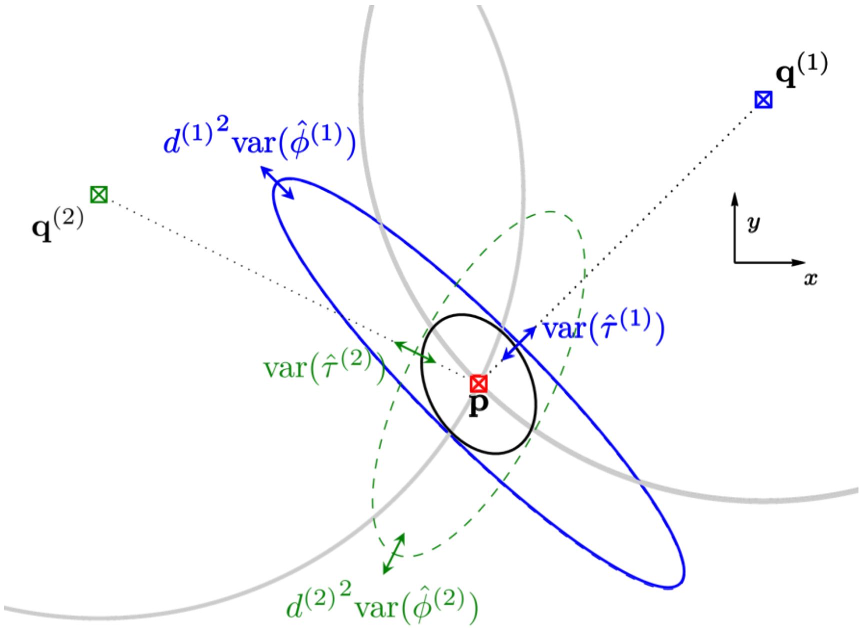

[T. Wilding, et al., "Accuracy bounds for array-based positioning in …," Sensors 2018, 18.]
[Witrisal et al. "Bandwidth Scaling and Diversity Gain for Ranging and Positioning in Dense Multipath Channels," IEEE Wireless Commun. Lett., 2016.]

Angle of arrival (AoA) estimation with antenna arrays

- Received signal (NB) :

$$\mathbf{r} = \mathbf{h}s + \mathbf{w}$$
$$= \alpha[e^{j2\pi f_c \tau_1(\phi_0)}, e^{j2\pi f_c \tau_2(\phi_0)}, \cdots, e^{j2\pi f_c \tau_M(\phi_0)}]^{\mathrm{T}} s + \mathbf{w}$$

- MF estimation:

$$\hat{\phi} = \arg\max_{\phi} |\mathbf{a}^{\mathrm{H}}(\phi)\mathbf{r}|$$

  - array response vector

$$\mathbf{a}(\phi) = [e^{j2\pi f_c \tau_1(\phi)}, e^{j2\pi f_c \tau_2(\phi)}, \cdots, e^{j2\pi f_c \tau_M(\phi)}]^{\mathrm{T}}$$

Scenario:

- 1 TX antenna (in direction ϕ)
- *M* RX antennas:

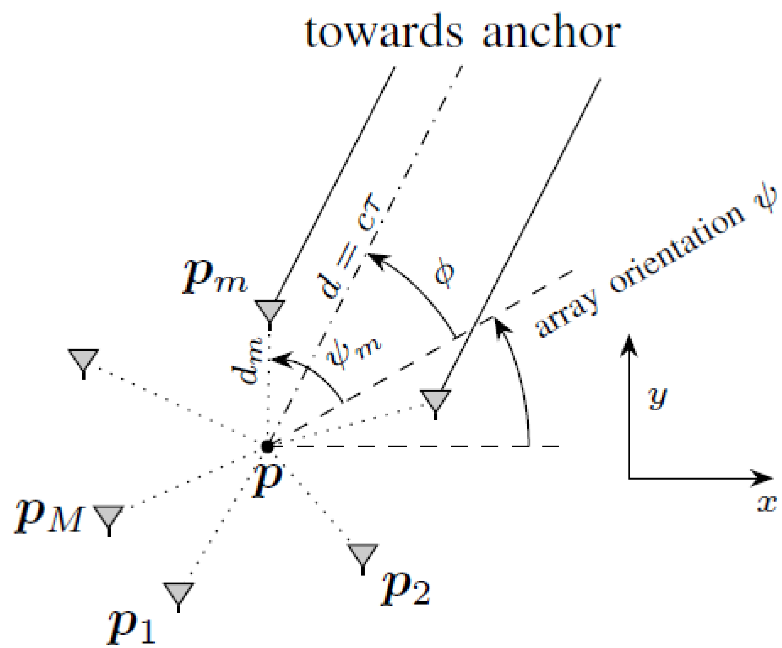

CRLB for **angle** estimation (phased array)

AWGN only

$$r_m(t) \approx \alpha e^{-j2\pi f_c \tau_m} s(t) + w(t)$$

AWGN + dense multipath

$$r_m(t) \approx \alpha e^{-j2\pi f_c \tau_m} s(t) + \underline{(s * \nu_m)(t)} + w(t)$$

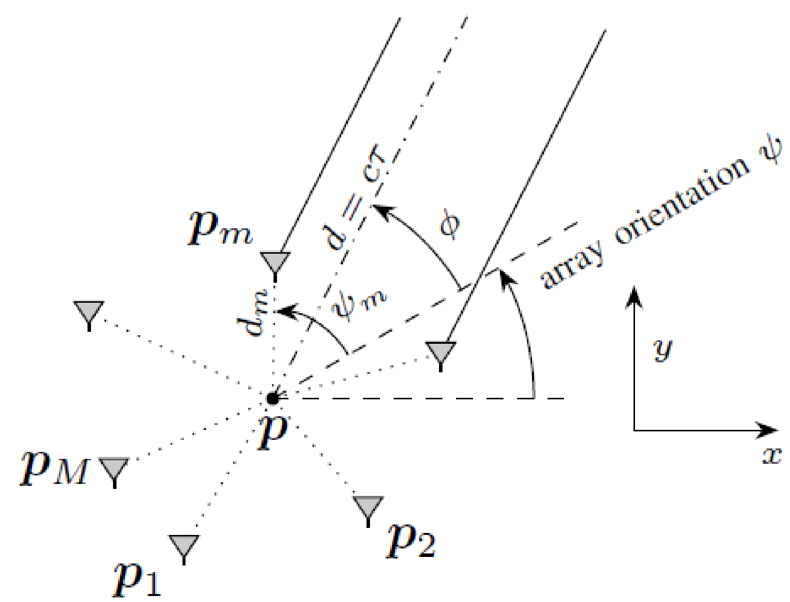

CRLB for AoA

$$\boxed{\mathrm{var}\{\hat{\phi}\} \gtrsim \left(8\pi^2 f_c^2 D^2(\phi) \mathrm{SNR}\right)^{-1}}$$

- squared effective aperture

$$D^2(\phi) = \sum_{m=1}^{M} \left[\frac{d_m}{c} \sin(\phi - \psi_m)\right]^2$$

- signal-to-noise ratio

$$\mathrm{SNR} = \frac{E_{\mathrm{LOS}}}{N_0}$$

➢ CRLB scales with f_c (carrier), **squared aperture** and SNR

➢ ***multipath interference*** limits the performance

[T. Wilding, et al., "AoA and ToA accuracy for antenna arrays in dense multipath channels," in ICL-GNSS, June 2018.]

Physically large arrays –
Performance scaling for angle estimation in dense multipath

- **CRLB for AoA**
  - uniform linear array (ULA)
  - **bandwidth** scales SINR

→ increase of array **aperture**

- **AoA estimators**
  - matched filter diverges from CRLB
  - **minimum SINR** needed for maximum likelihood

→ **detectability** improved

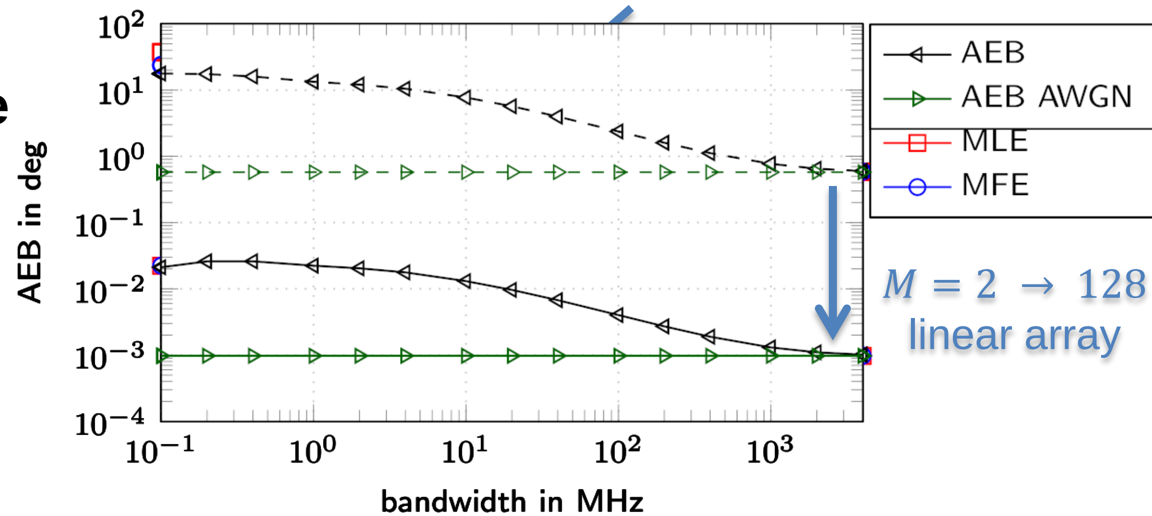

- Large arrays offer tremendous **accuracy gain!**
- **How to exploit it?**

Outline

- Introduction
- Ranging and positioning in dense multipath
  - Bandwidth scaling and MIMO gain
- **Sensing**
  - **Multipath-assisted indoor positioning**
  - **Environment modeling**
- Wireless Power Transfer
- Conclusions

Reliance on Line-of-Sight

Measurement of body influence (off-body channel)

Measurement Setup

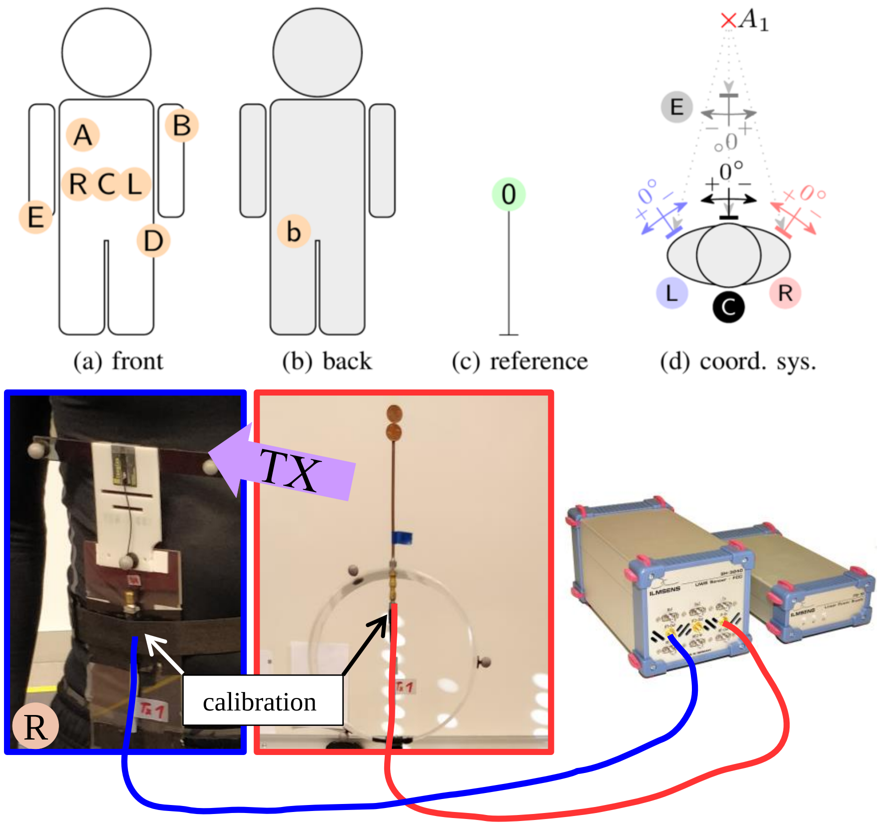

Characterization of LOS

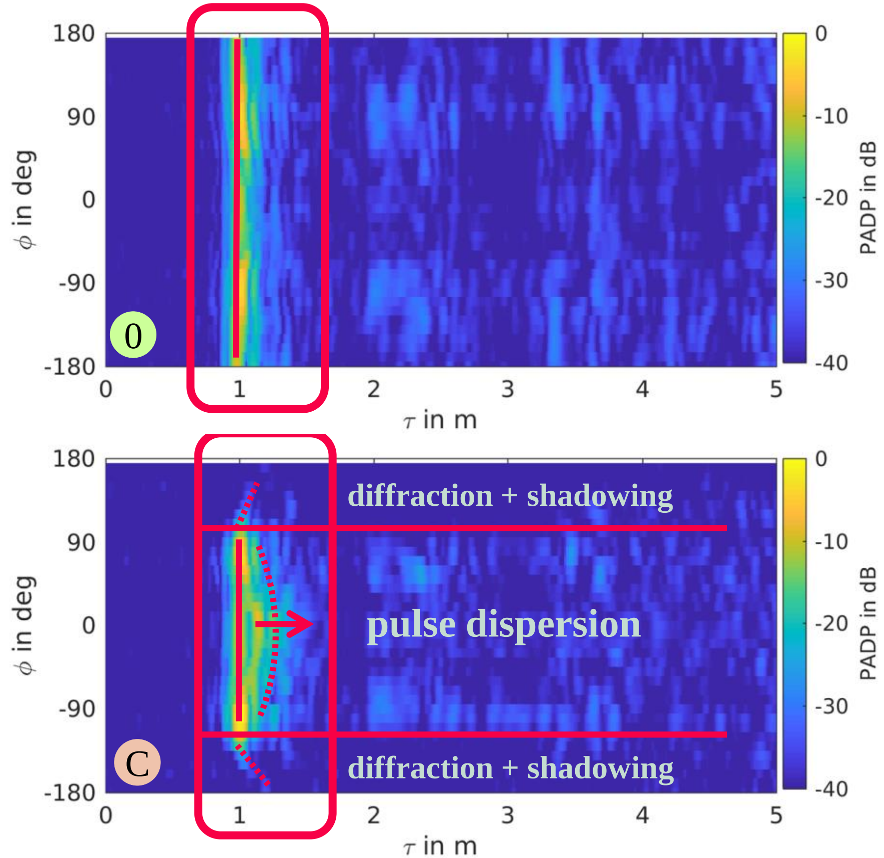

Reliance on Line-of-Sight

Impact of body shadowing

Walking along trajectory

- two fixed anchors

Ranging

- outliers

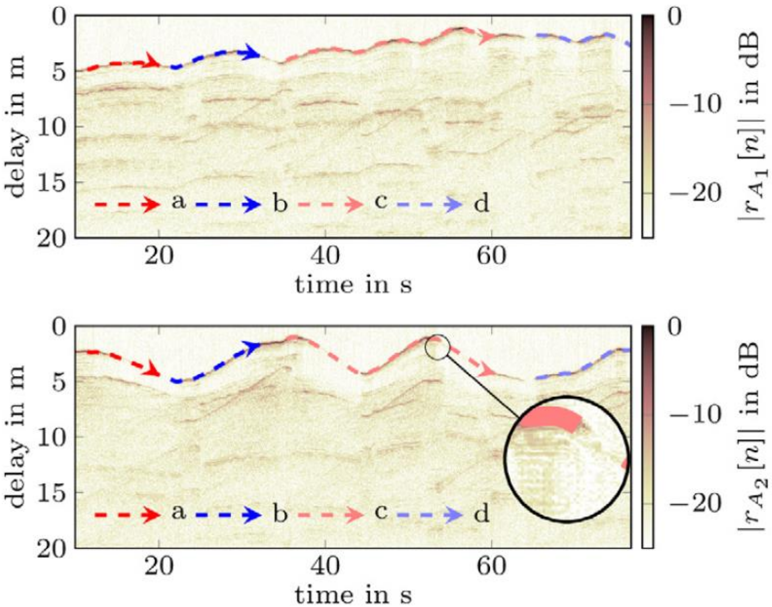

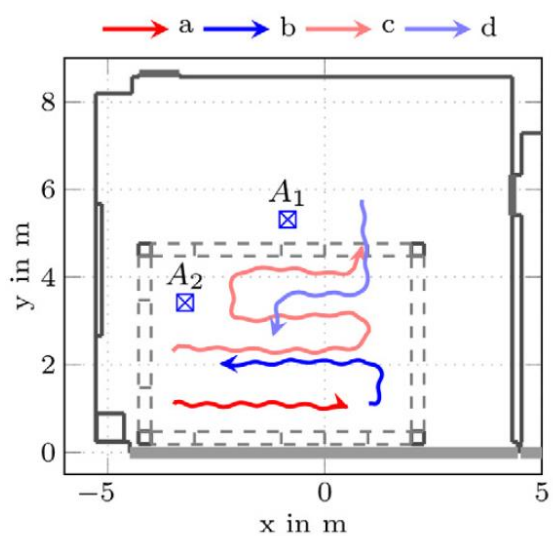

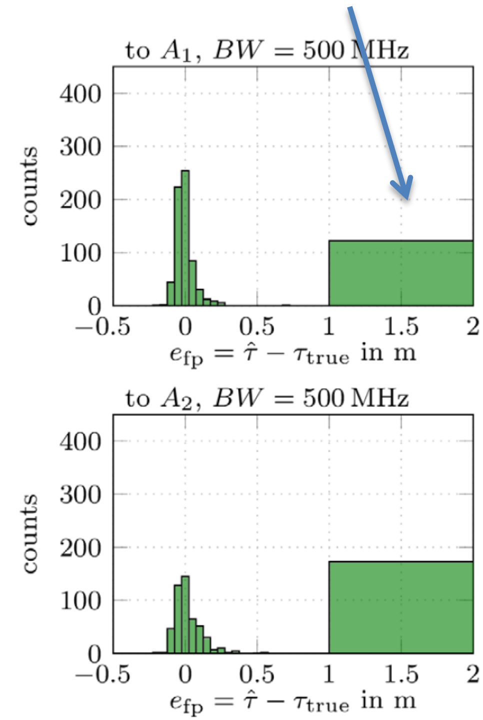

Multipath-assisted Indoor Navigation and Tracking (MINT) – *concept and geometric model*

- **Idea:**
  - exploit range/position information from *reflected* multipath
- **Benefits:**
  - less anchor nodes;
  - more redundancy, i.e. robustness in NLOS;
  - higher accuracy
- **Geometric model (GPEM)**: *virtual anchors (VAs)* (mirror sources)

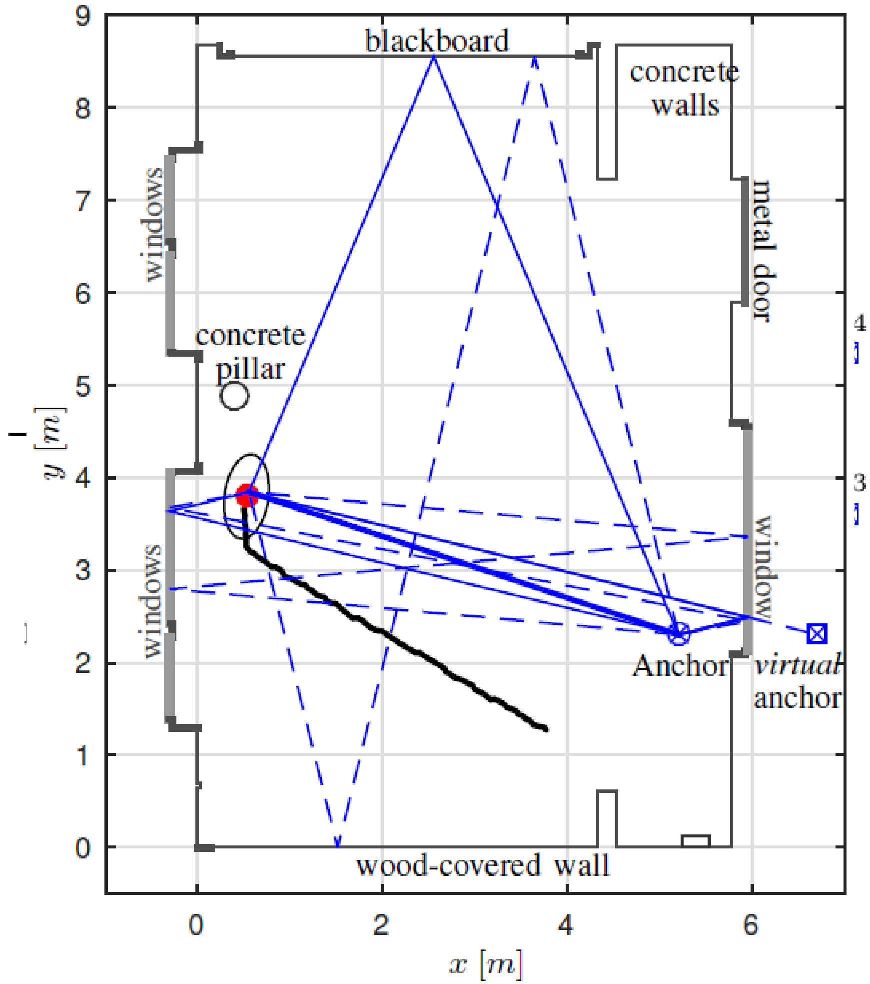

[Meissner, Steiner, Witrisal, "UWB Positioning with Virtual Anchors and Floor Plan Information," in WPNC, Dresden, March 2010.]

Signal Model

(Geometry-based stochastic channel model - GSCM)

- Received signal: ($s(t)$: TX signal)

$$r(t) = \underbrace{\sum_{k=1}^{K} \alpha_k s(t-\tau_k)}_{\text{useful signal}} + \underbrace{\int_{-\infty}^{\infty} s(\lambda)\nu(t-\lambda)d\lambda}_{\text{interference}} + \underbrace{w(t)}_{\text{noise}}$$

  - *K* **deterministic** multipath components
    - Anchor (LOS), virtual anchors (NLOS), deterministic scatterers
  - **Diffuse** multipath *v*(*t*)
    - PDP $S_\nu(\tau)$
- **MPCs** characterized by

$$\mathrm{SINR}_k := \frac{|\alpha_k|^2}{N_0 + T_s S_\nu(\tau_k)}$$

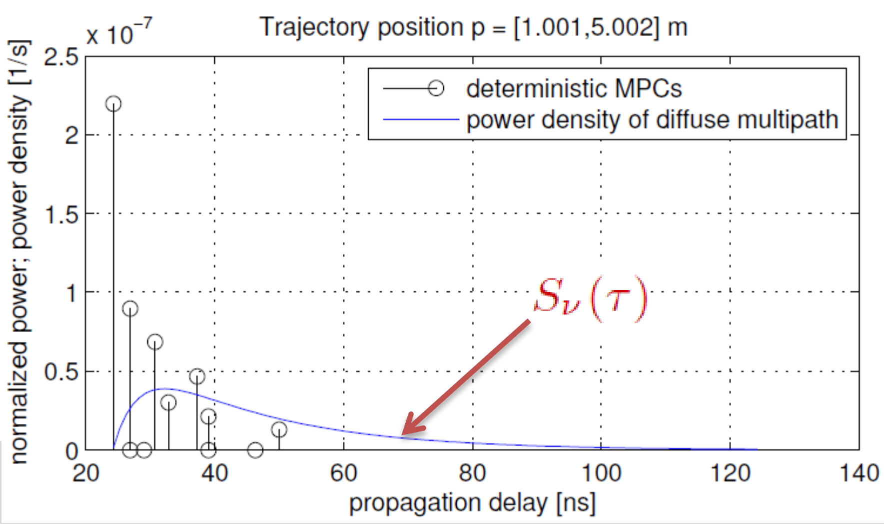

Position error bound for MINT
(Cramér-Rao lower bound derived from LHF)

- *Position error variance* is bounded by $\mathrm{var}\{\hat{\mathbf{p}}\} \geq \mathrm{tr}\{\mathbf{J}_{\mathbf{p}}^{-1}\}$
  - If no "path-overlap" occurs (orthogonal signals from VAs)

$$\mathbf{J}_{\mathbf{p}} = \frac{8\pi^2\beta^2}{c^2} \sum_{k=1}^{K} \mathrm{SINR}_k \mathbf{J}_{\mathbf{r}}(\phi_k)$$

- **effective** SINR$_k$ determines **ranging information intensity**
  - for MPC from k-th virtual anchor

$$\mathrm{SINR}_k := \frac{|\alpha_k|^2}{N_0 + T_{\mathrm{s}} S_\nu(\tau_k)}$$

- **Ranging direction** matrix accounts for geometry

[Leitinger, et al., "Evaluation of Position-related Information in Multipath Components for Indoor Positioning," IEEE JSAC, 2015.]

Multipath-resolved **environment model**

- Exploit (specular) multipath components and location
  - Environment model: **predictability** of multipath
  - Yields **robust tracking** (here)

Geometric model:

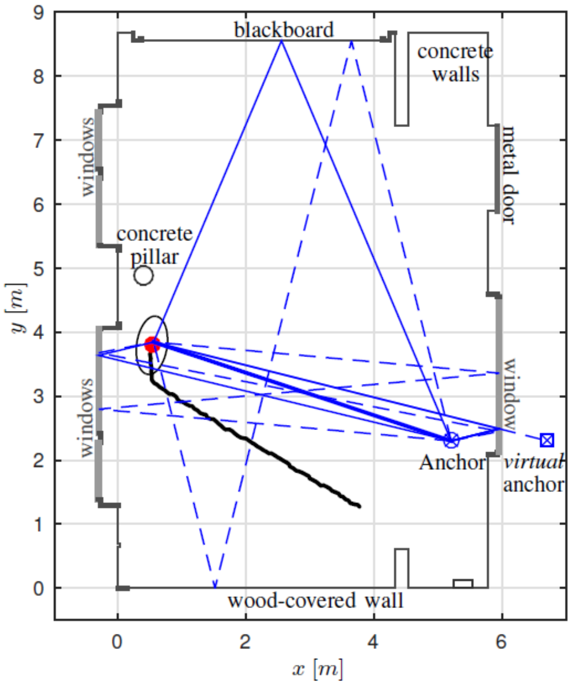

Signals / Quality (SINR):

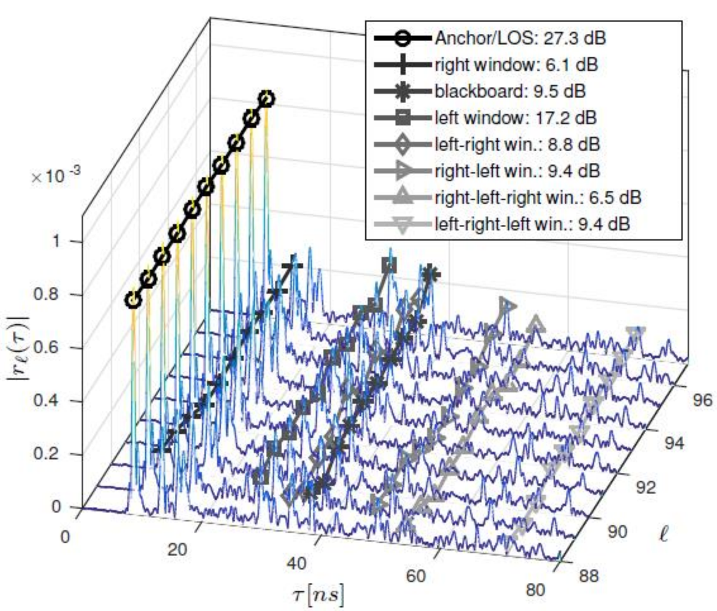

Environment model:

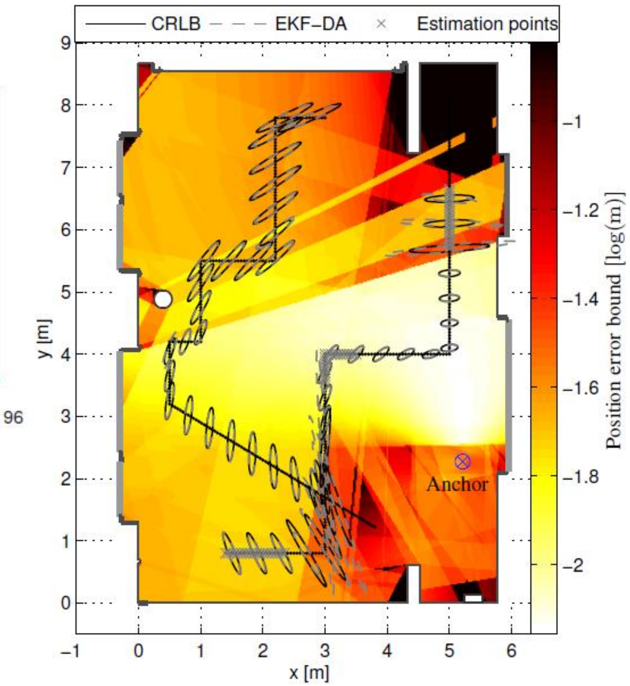

[Witrisal, et al., "High-Accuracy Localization for Assisted Living," IEEE Signal Processing Mag., March 2016.]

Tracking algorithms exploiting multipath

- (0) multipath parameters (ToA/AoA) estimated from **received signals**
- (1) ***data association*** of multipath ranges and *state-space tracking*
- (2) **ranging uncertainty** is estimated from multipath amplitudes
- (3) a **SLAM**-style algorithm is used to *discover new VAs*

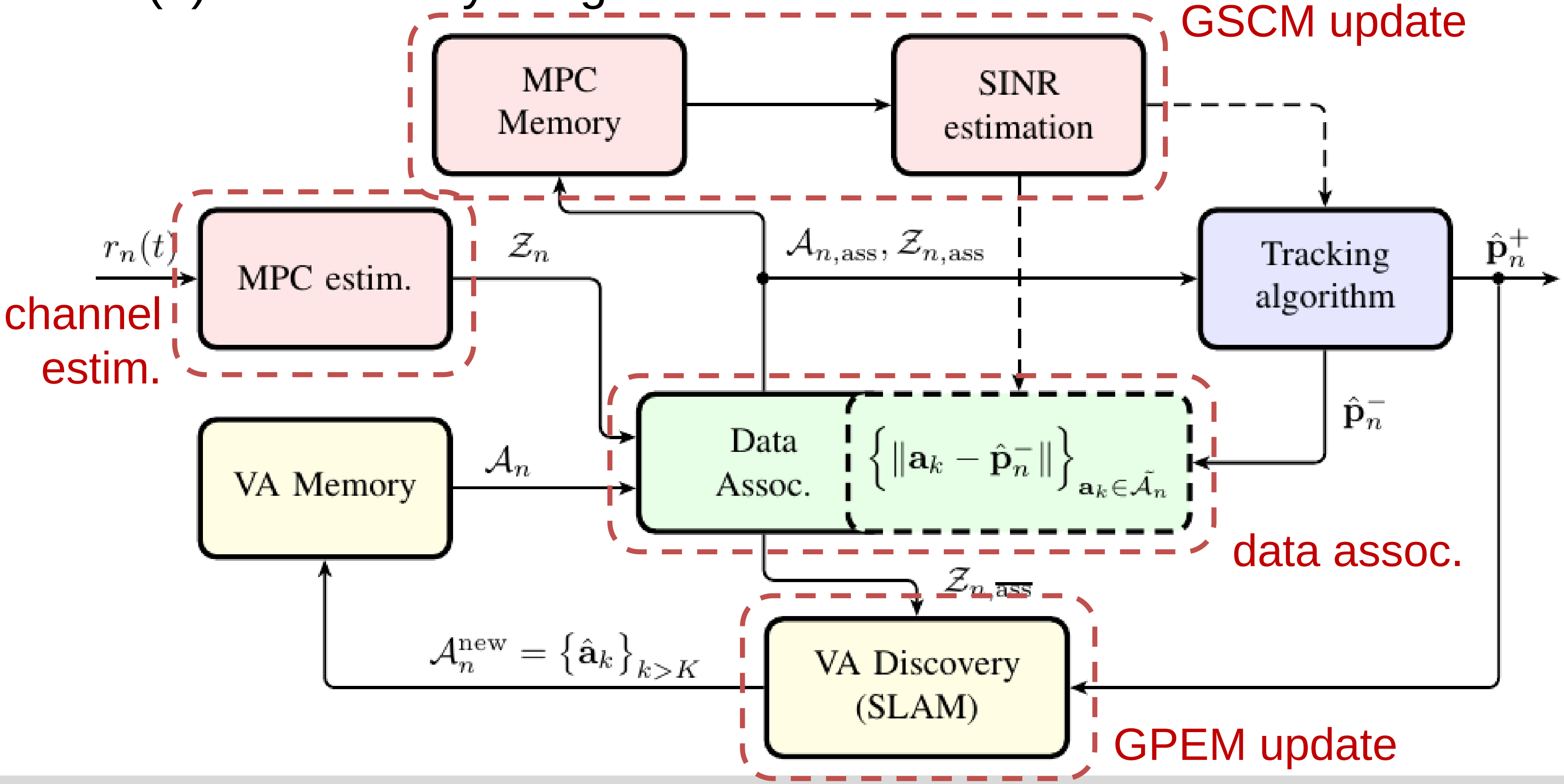

[Meissner, Witrisal, et al., "UWB for Robust Indoor Tracking: […]," IEEE Wireless Commun. Lett., 2014.]
[Leitinger, et al., " A Belief Propagation Algorithm for Multipath-Based SLAM,“ IEEE TWC, 2019.]
[Witrisal, et al., "High-Accuracy Localization for Assisted Living,“ IEEE Signal Processing Mag., March 2016.]

Multipath-based SLAM

Baysian inference on factor graph

PF: potential feature

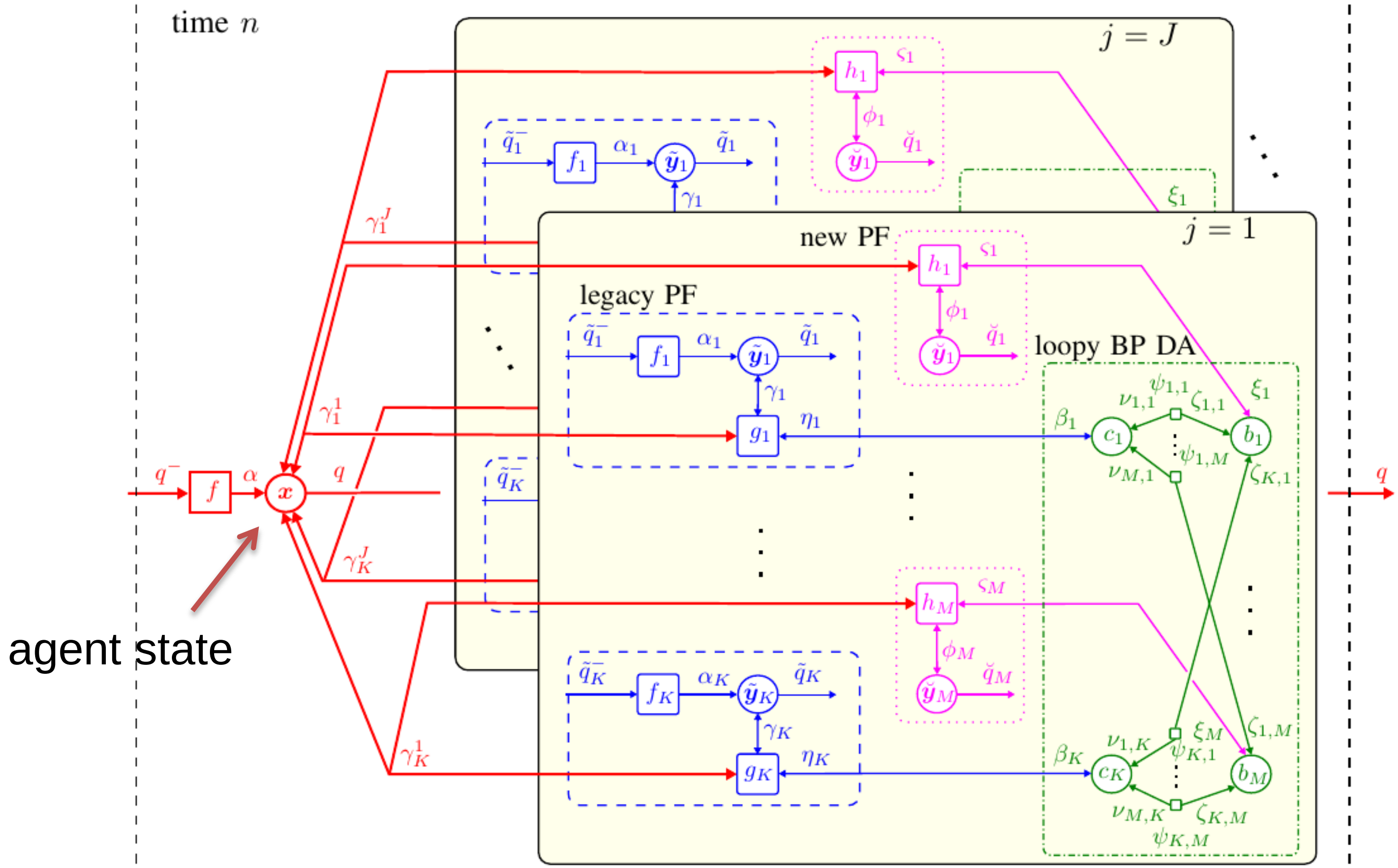

[Leitinger, et al., "A Belief Propagation Algorithm for Multipath-Based SLAM," IEEE TWC, 2019.]

Multipath-based SLAM – range-only

Particle convergence

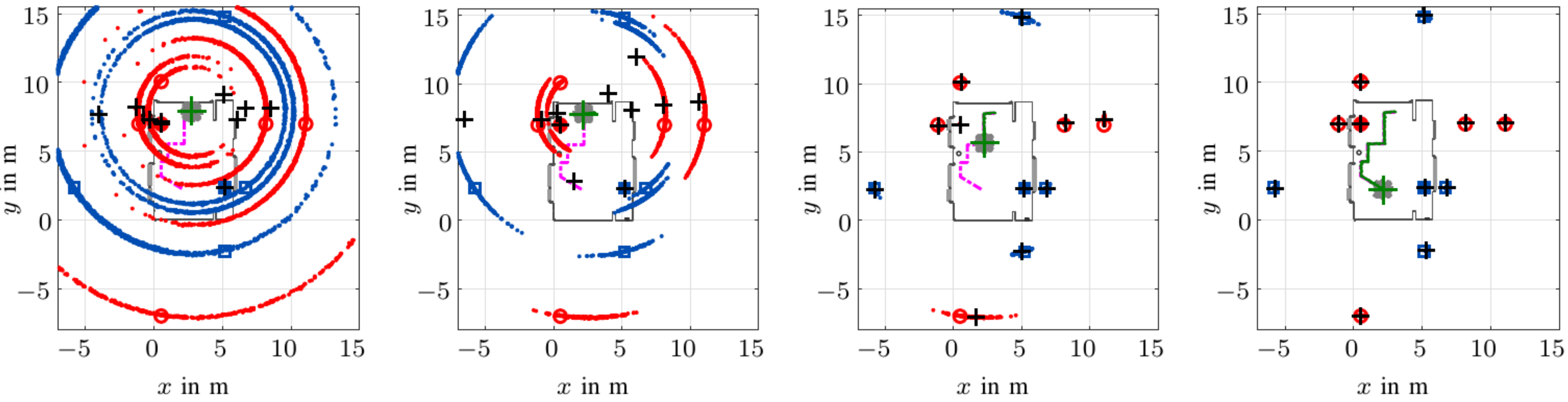

For real data:

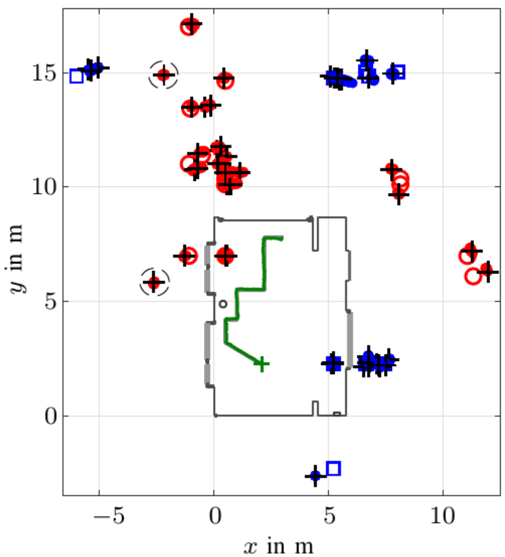

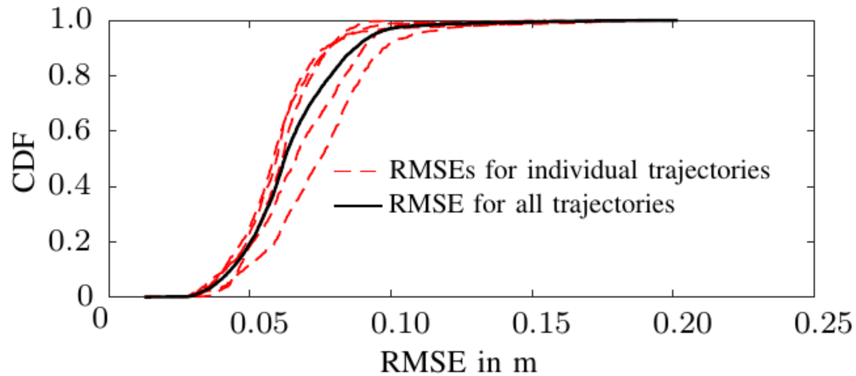

[Leitinger, et al., "A Belief Propagation Algorithm for Multipath-Based SLAM," IEEE TWC, 2019.]

Environment sensing with physically large array

2.4 m x 1.6 m virtual array measurement (8400 elements) @ 7 GHz

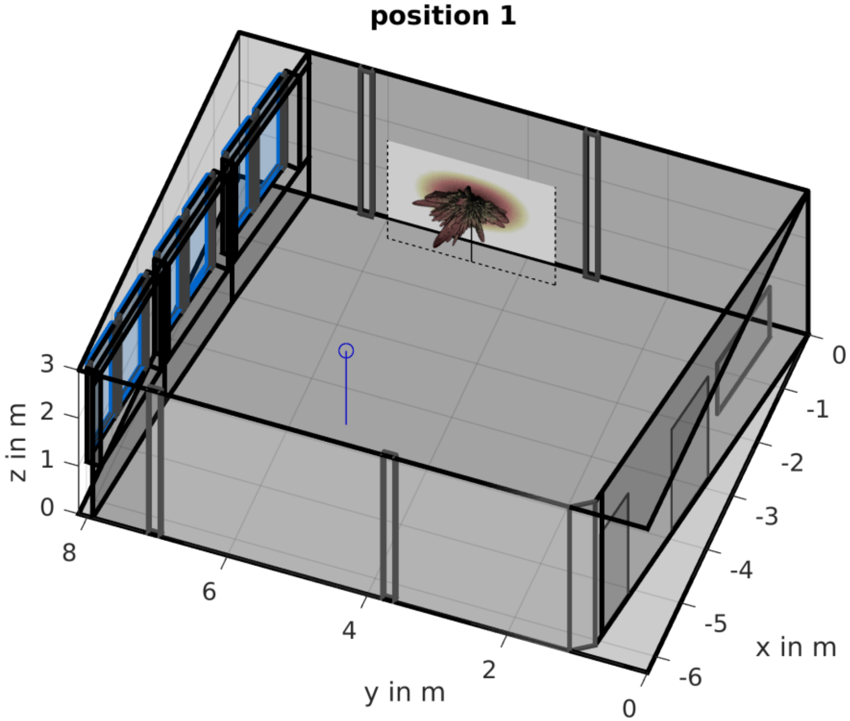

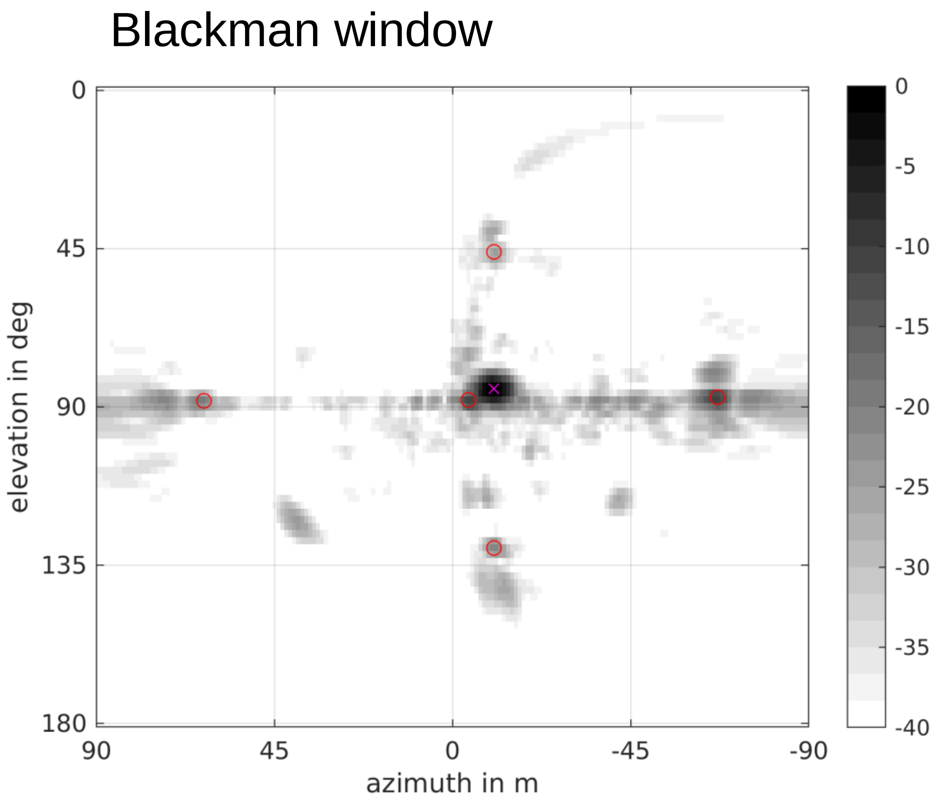

[Illustration: Thomas Wilding, Benjamin Deutschmann]

Channel Parameter Estimation

Utilizing Sparse Bayesian Learning

Measured data:

- 3x3 antenna array (2cm spacing)
- Pulse RRC
  - pulse duration 1 ns; roll-off-factor 0.6; center frequency 6 GHz
- AWGN: 30 dB SNR
- **DMC: Double exponential PDP**

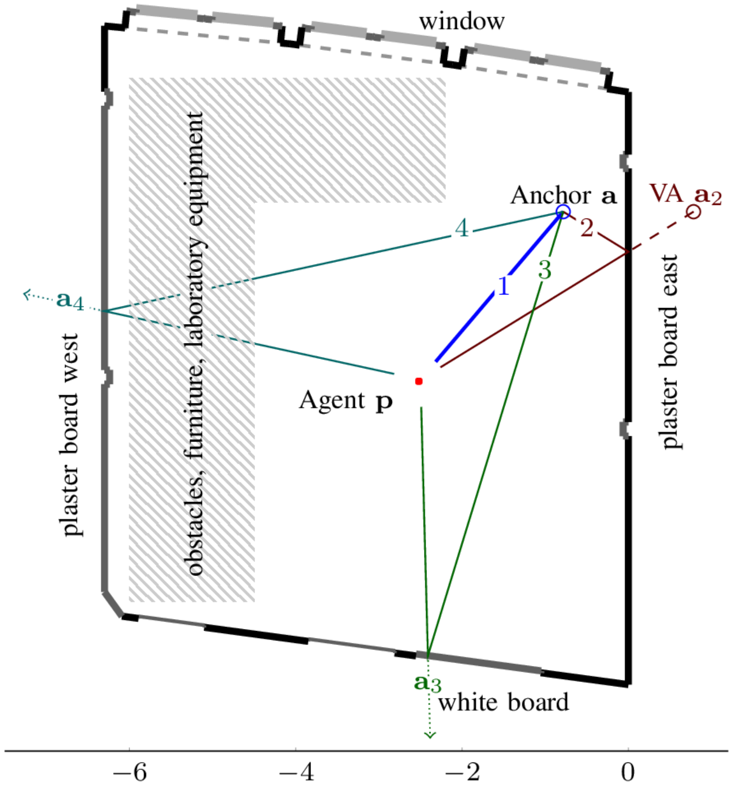

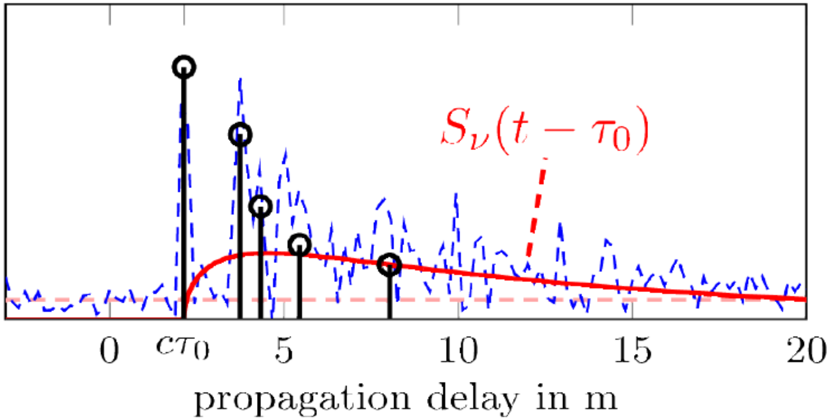

[Grebien, Leitinger, Fleury, et al., "Sparse Bayesian Variational Multipath Channel Estimation Considering Dense Multipath," IEEE Trans., 2020, under preparation.]

Channel Parameter Estimation

Utilizing Sparse Bayesian Learning

Probability of Artifact and Probability of Detection - ROC

- Single component in DMC plus AWGN

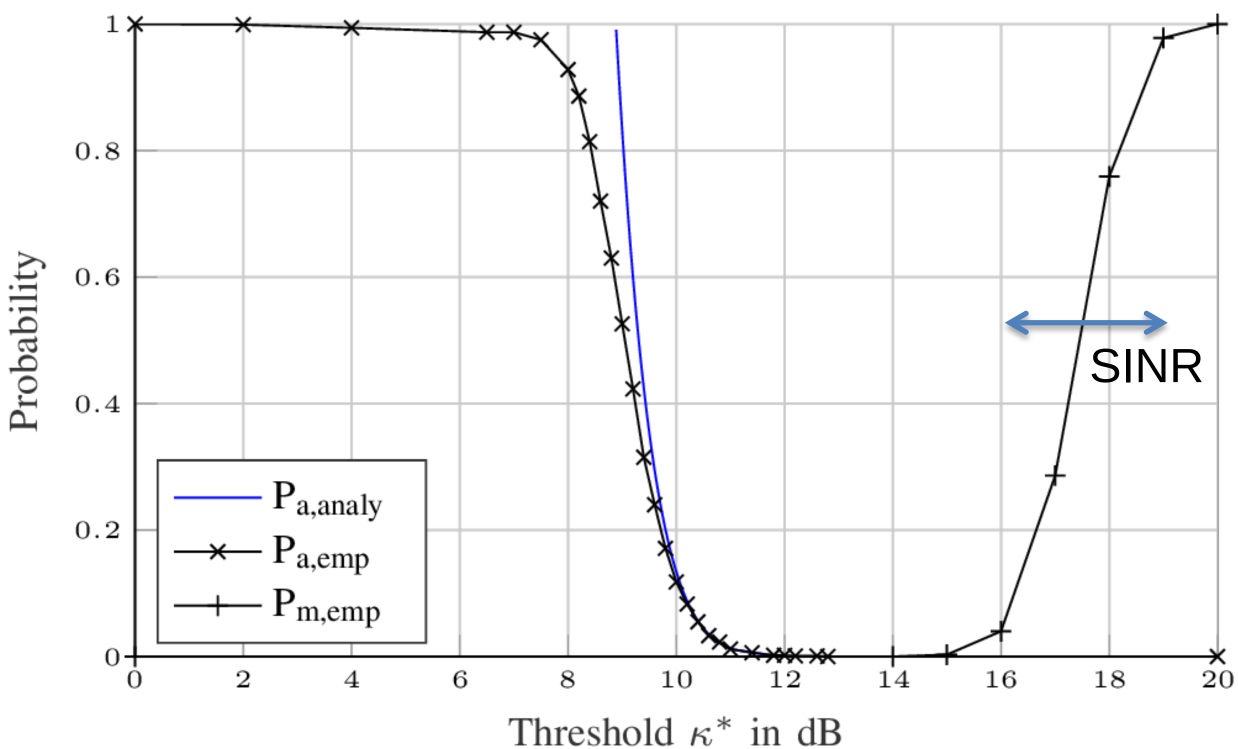

[Grebien, Leitinger, Fleury, et al., "Sparse Bayesian Variational Multipath Channel Estimation Considering Dense Multipath," IEEE Trans., 2020, under preparation.]

Channel Parameter Estimation

Utilizing Sparse Bayesian Learning

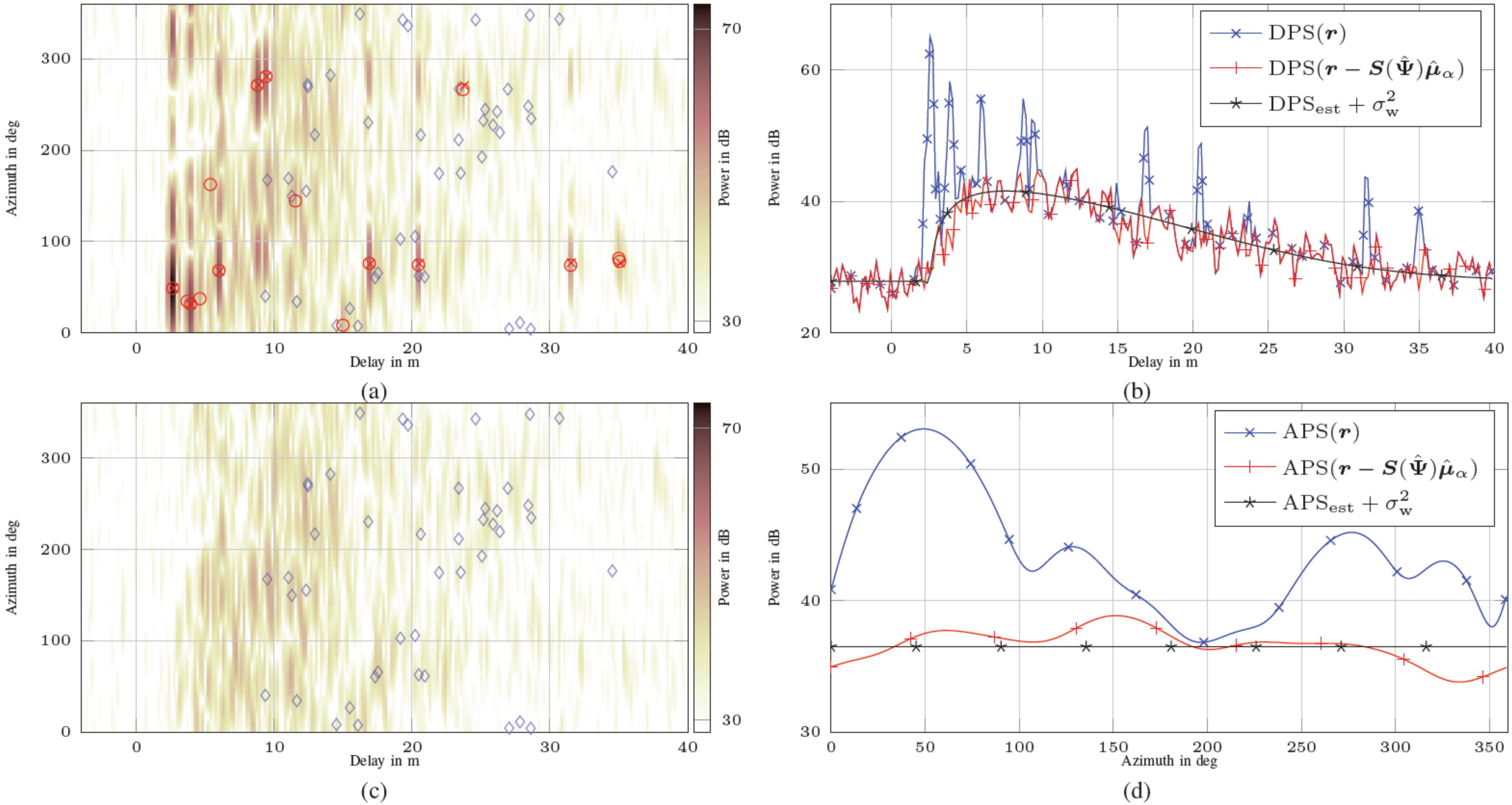

[Grebien, Leitinger, Fleury, et al., "Sparse Bayesian Variational Multipath Channel Estimation Considering Dense Multipath,“ IEEE Trans., 2020, under preparation.]

Outline

- Introduction
- Ranging and positioning in dense multipath
  - Bandwidth scaling and MIMO gain
- Sensing
  - Multipath-assisted indoor positioning
  - Environment modeling
- **Wireless Power Transfer**
  - **With physically large arrays**
- Conclusions

Physically Large Antennas/Arrays – What's different?

User in "far field"

- **Plane wave**
- $d \gg d_F$ … Fraunhofer distance

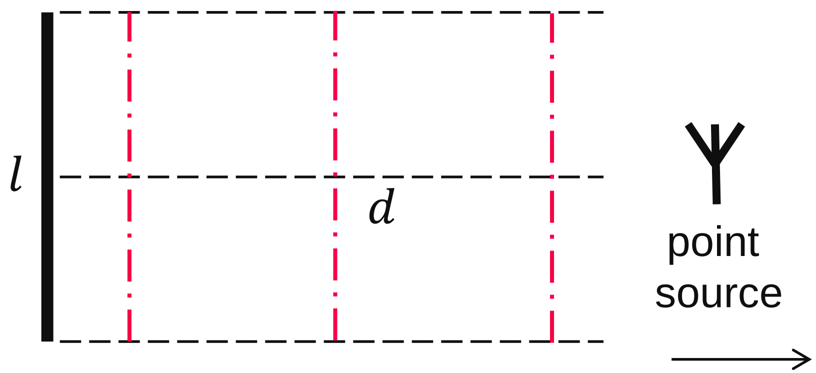

- Field distribution: $E, H \propto \frac{1}{d} f(\theta, \phi)$
  - Radiation pattern

User in **"near field"**

- Spherical wave
- $d \leq d_F = 2\, l^2/\lambda$

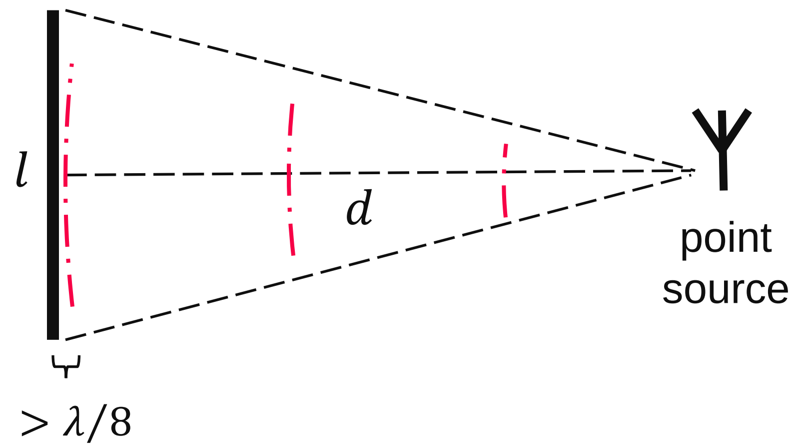

- Field distribution: $E, H = f(d, \theta, \phi)$
  - Distance dependent → focusing

Physically Large Arrays

Example: user in "near field" $d_{FA} = 2l^2/\lambda$

frequency f_c	wavelength λ	array length l	**Fraunhofer distance d_{FA}**
2.4 GHz	12.5 cm	2.5 m = 20 λ	**100 m**
6 GHz	5 cm	2.5 m = 50 λ	**250 m**

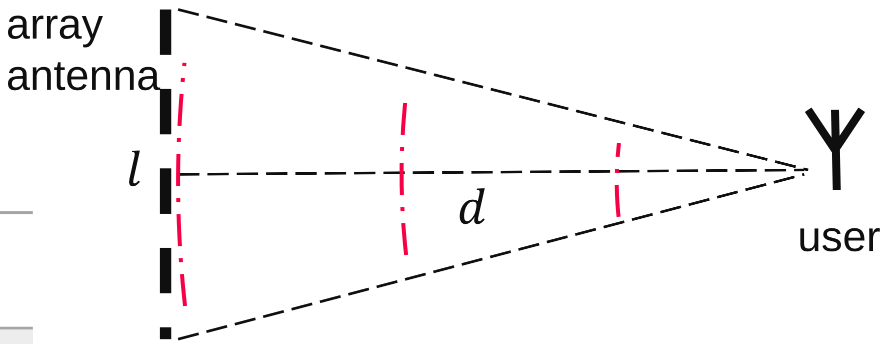

Beam focusing – width of focal point

- $w = d\,{}^{\lambda}/_{l}$

wavelength λ	distance d	array length l	**focal point w**
12.5 cm	6 m	2.5 m	**30 cm**
5 cm	6 m	2.5 m	**12 cm**

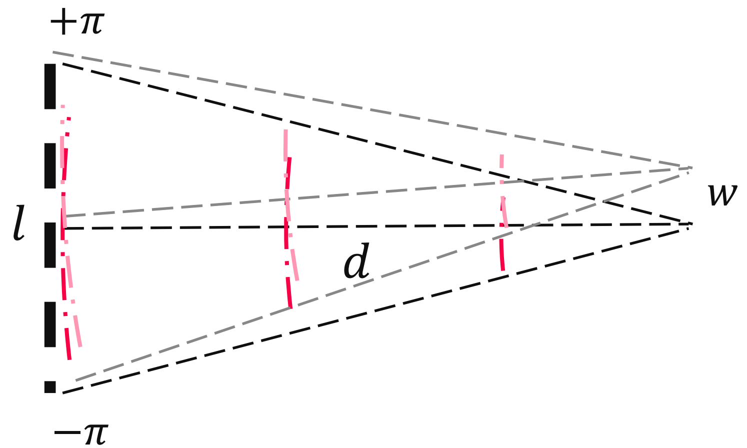

Beam focusing: user in the near field (@ 2.4 GHz)

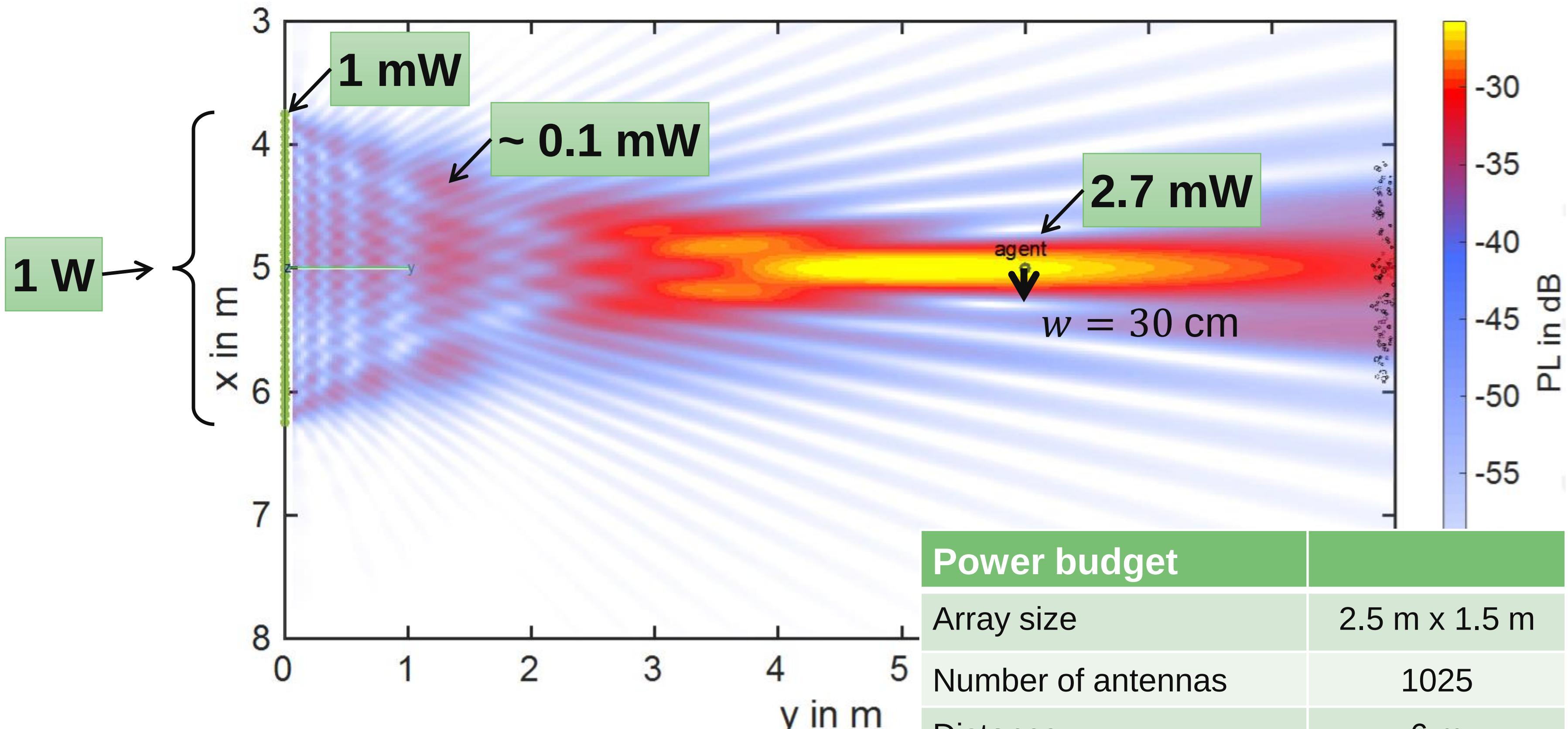

Power converges towards user:
a radical shift

Power budget	
Array size	2.5 m x 1.5 m
Number of antennas	1025
Distance	6 m
Single-antenna path loss	55.6 dB
Array gain	30.1 dB
Array path loss (simul.)	**25.7 dB**

[Illustration: Benjamin Deutschmann]

Beam focusing: user in the **far field (@ 24 GHz)**

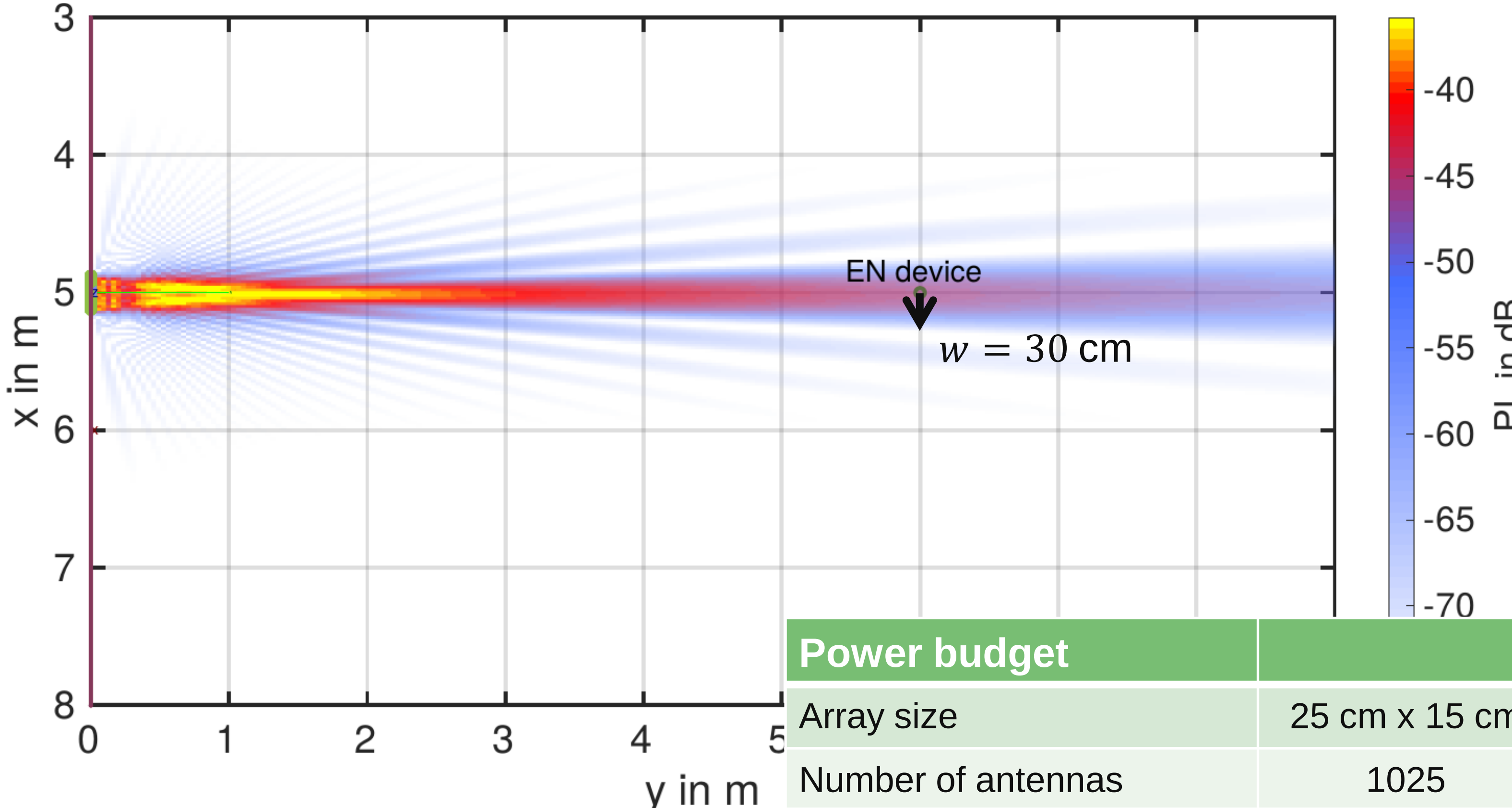

Power budget	
Array size	25 cm x 15 cm
Number of antennas	1025
Distance	6 m
Single-antenna path loss	75.6 dB
Array gain	30.1 dB
Array path loss	**45.5 dB**

Conventional situation:
Power diverges from array

[Illustration: Benjamin Deutschmann]

Channel Modeling for physically large arrays

Illustration of propagation mechanisms

Simulation environment:

- Specular reflections (virtual arrays)
- Scatter points

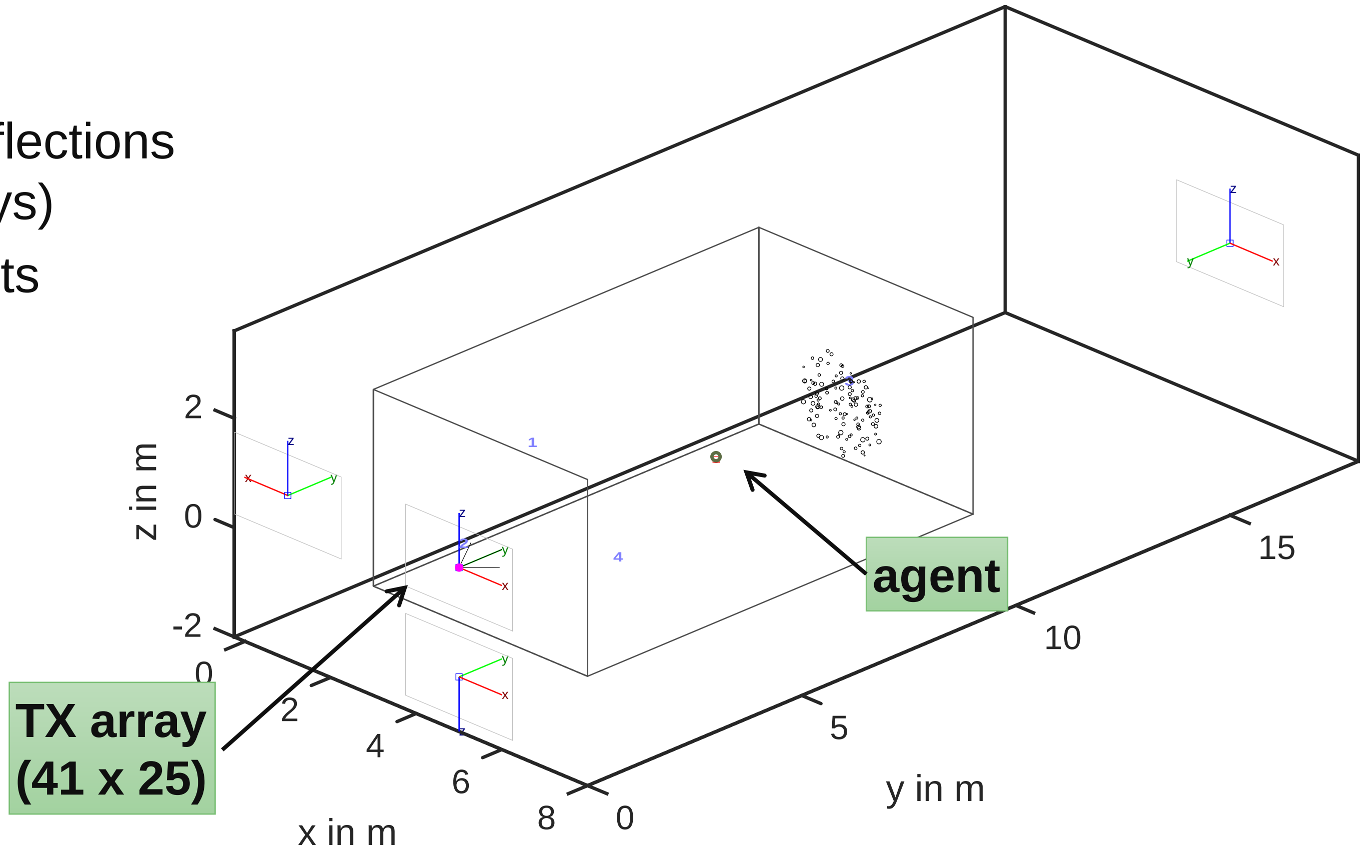

[Illustration: Benjamin Deutschmann]

Line-of-sight only

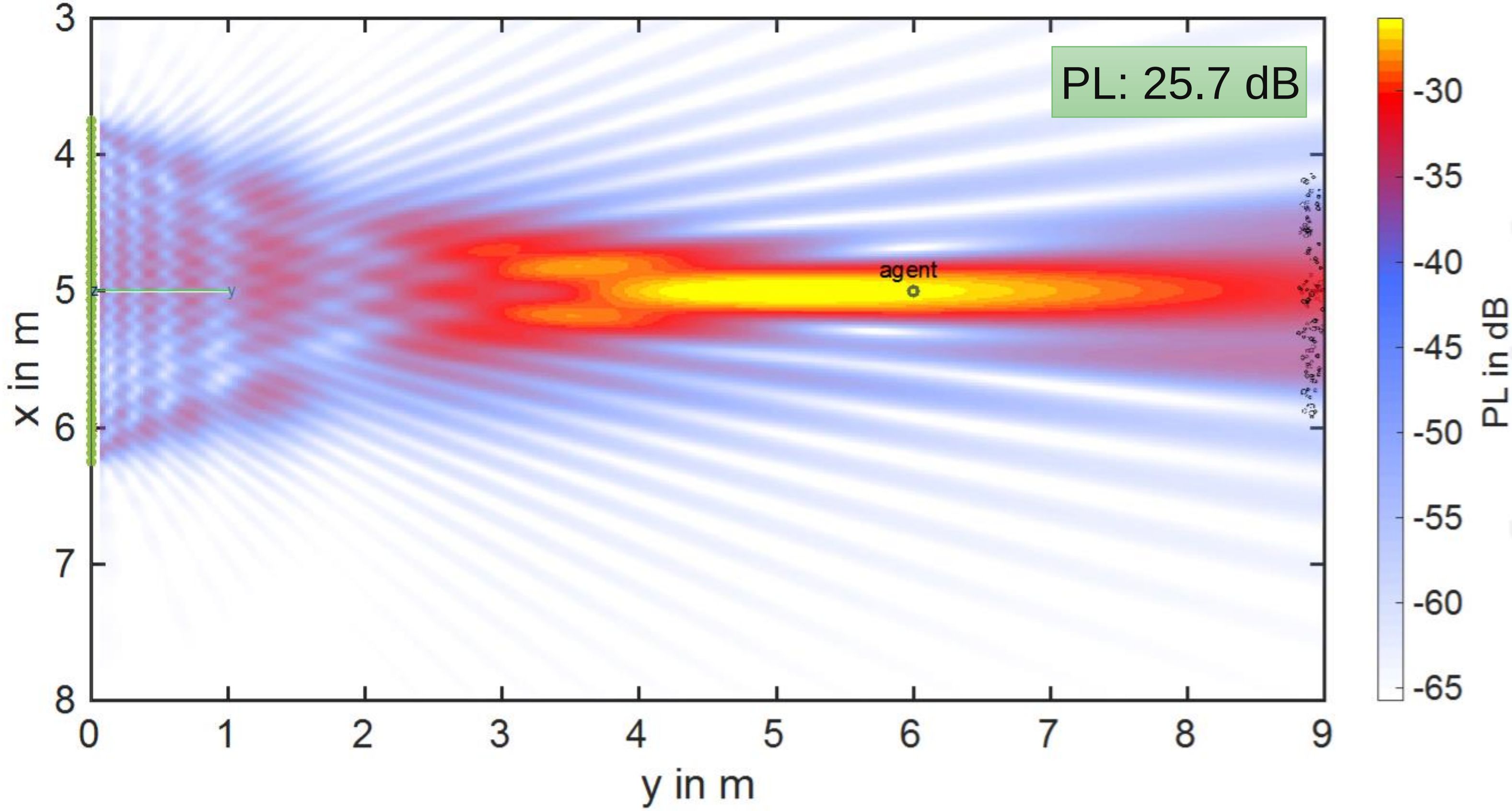

[Illustration: Benjamin Deutschmann]

Line-of-sight + **one specular component**

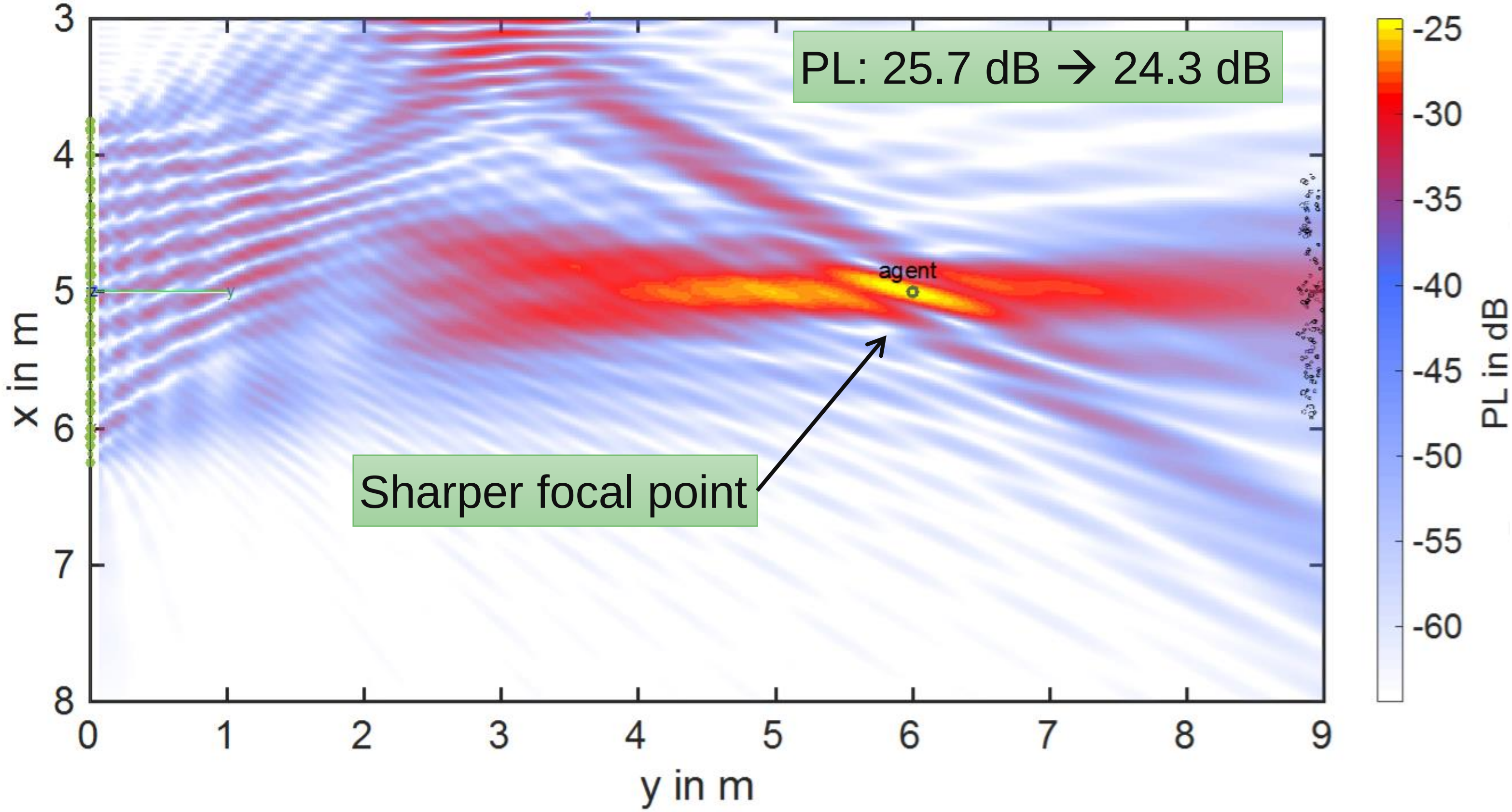

[Illustration: Benjamin Deutschmann]

Line-of-sight + 1 Wall + Floor (2 specular components)

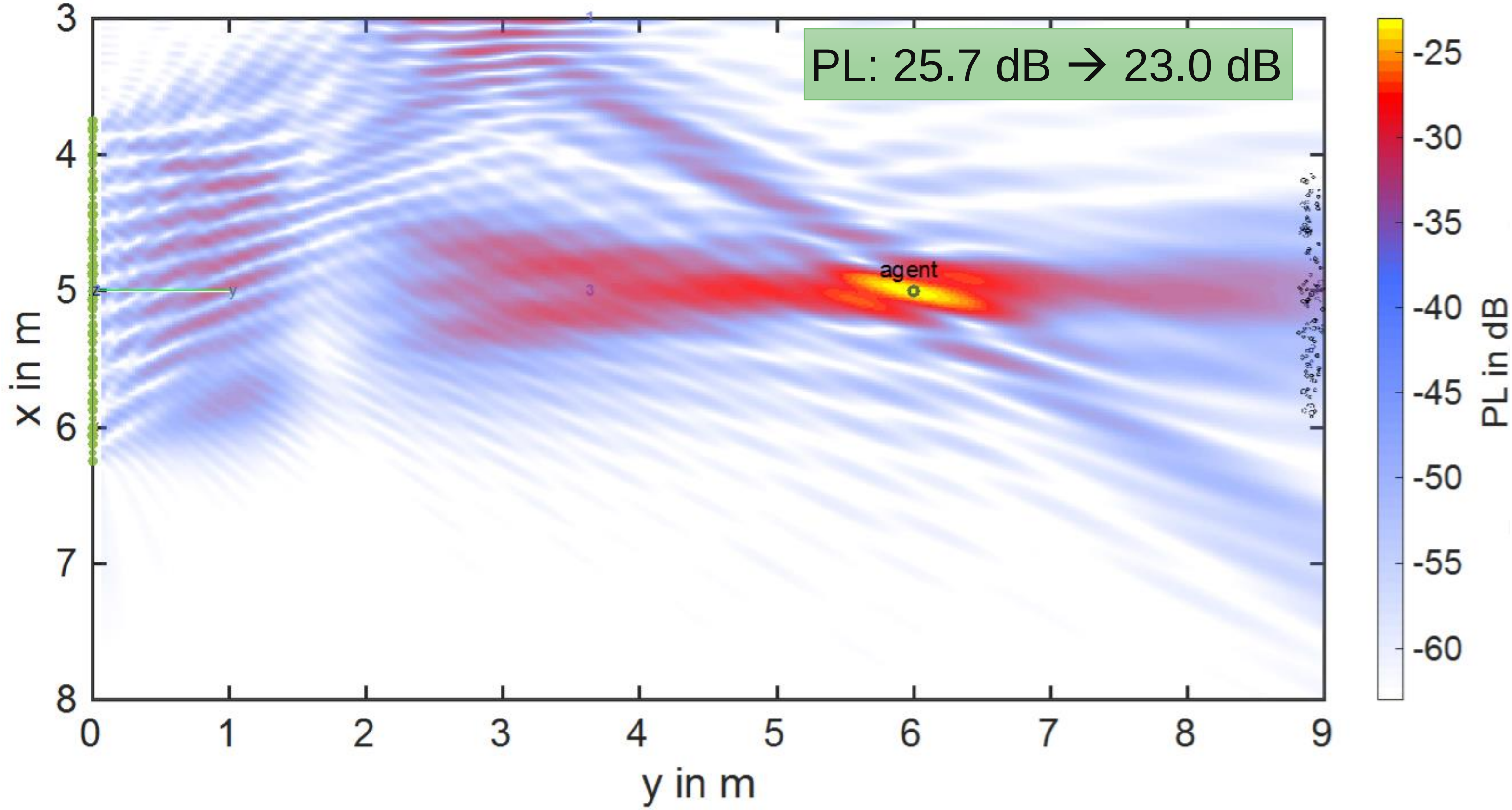

[Illustration: Benjamin Deutschmann]

Line-of-sight + **facing wall**

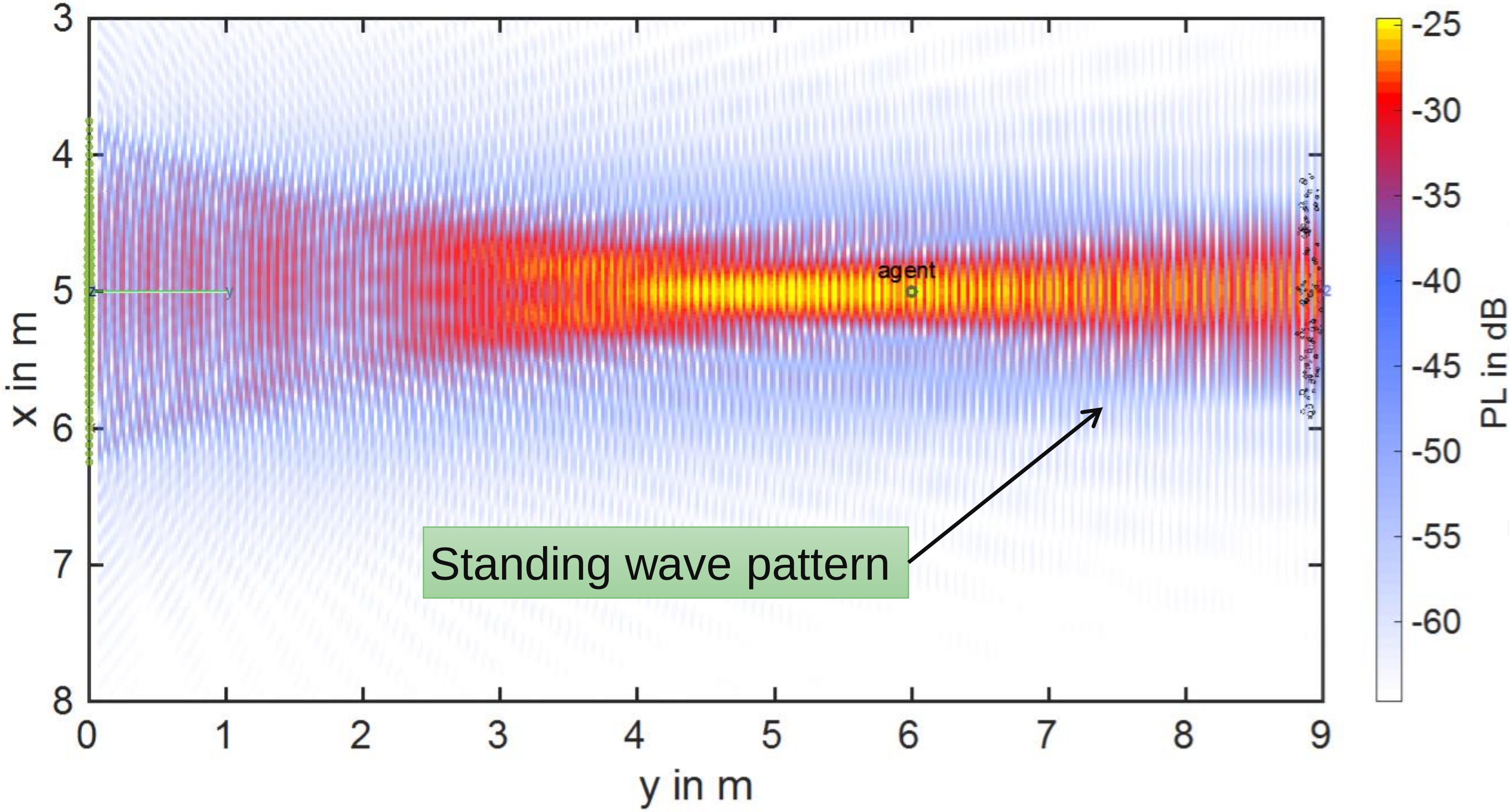

[Illustration: Benjamin Deutschmann]

Complete example (LOS + 3 SMCs + scattering)

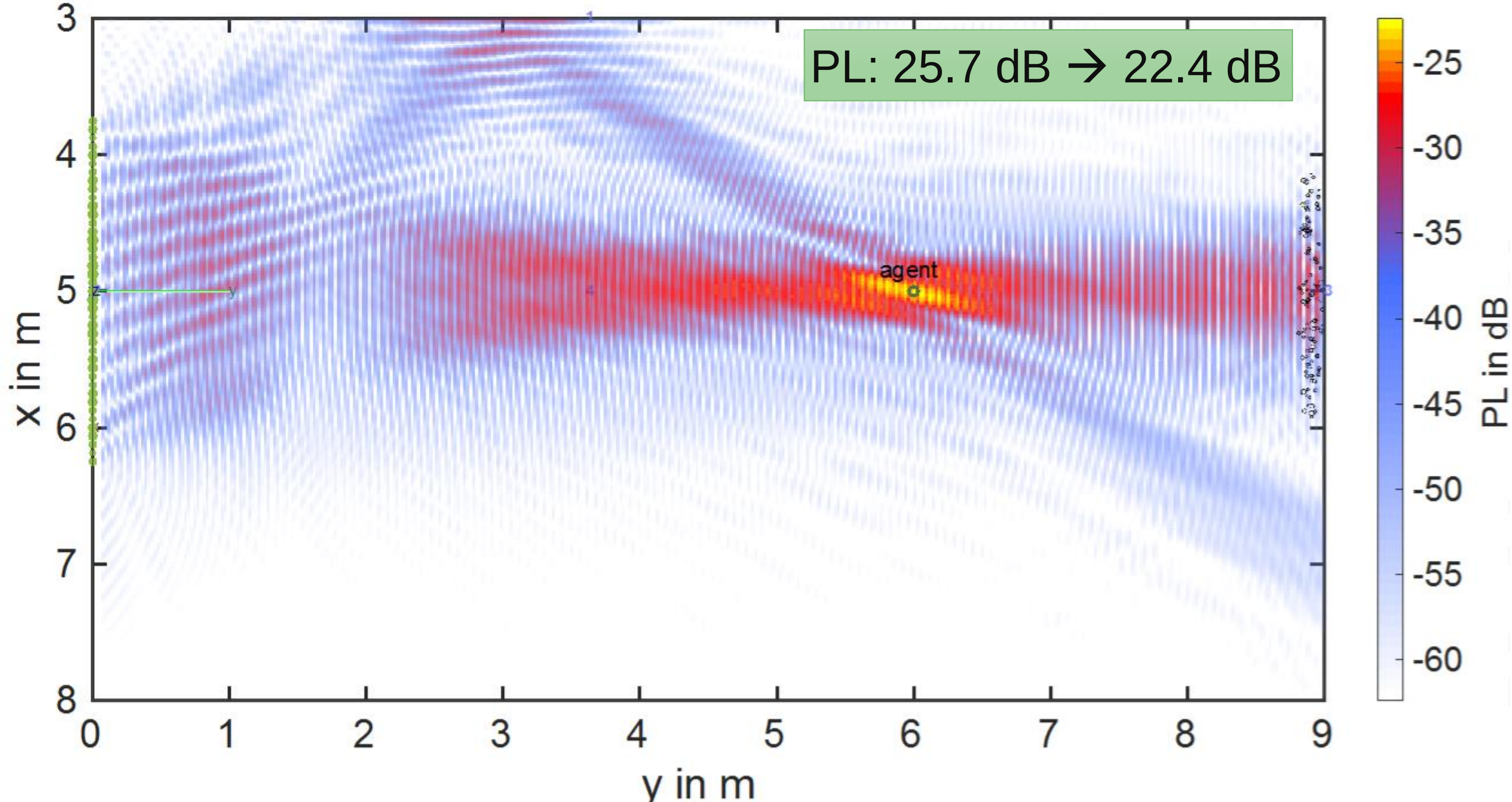

Specular multipath components **enhance** the focusing

[Illustration: Benjamin Deutschmann]

Example 2: Line-of-sight + **scatter points**

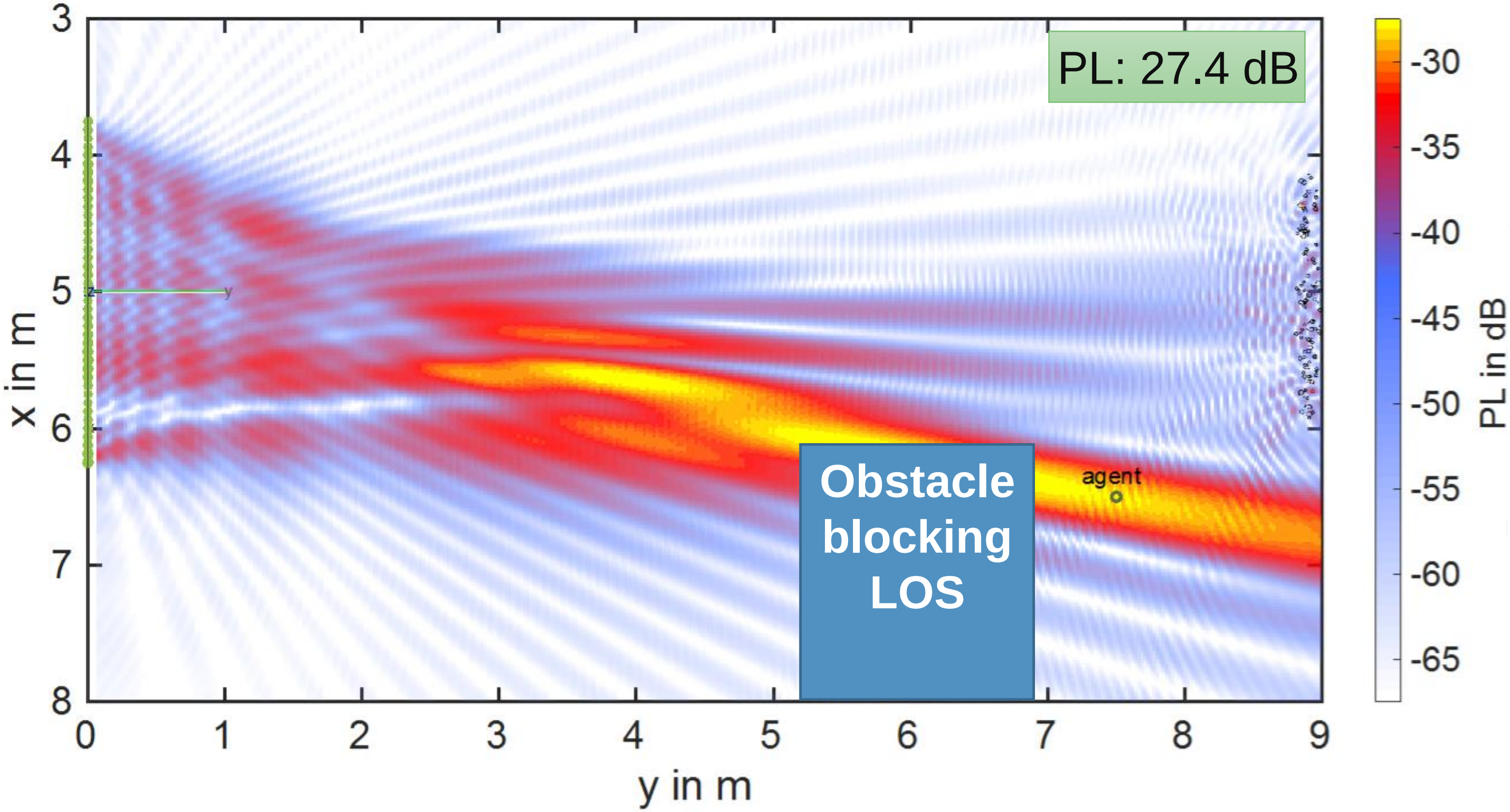

[Illustration: Benjamin Deutschmann]

Line-of-sight **blocked** + scatter points

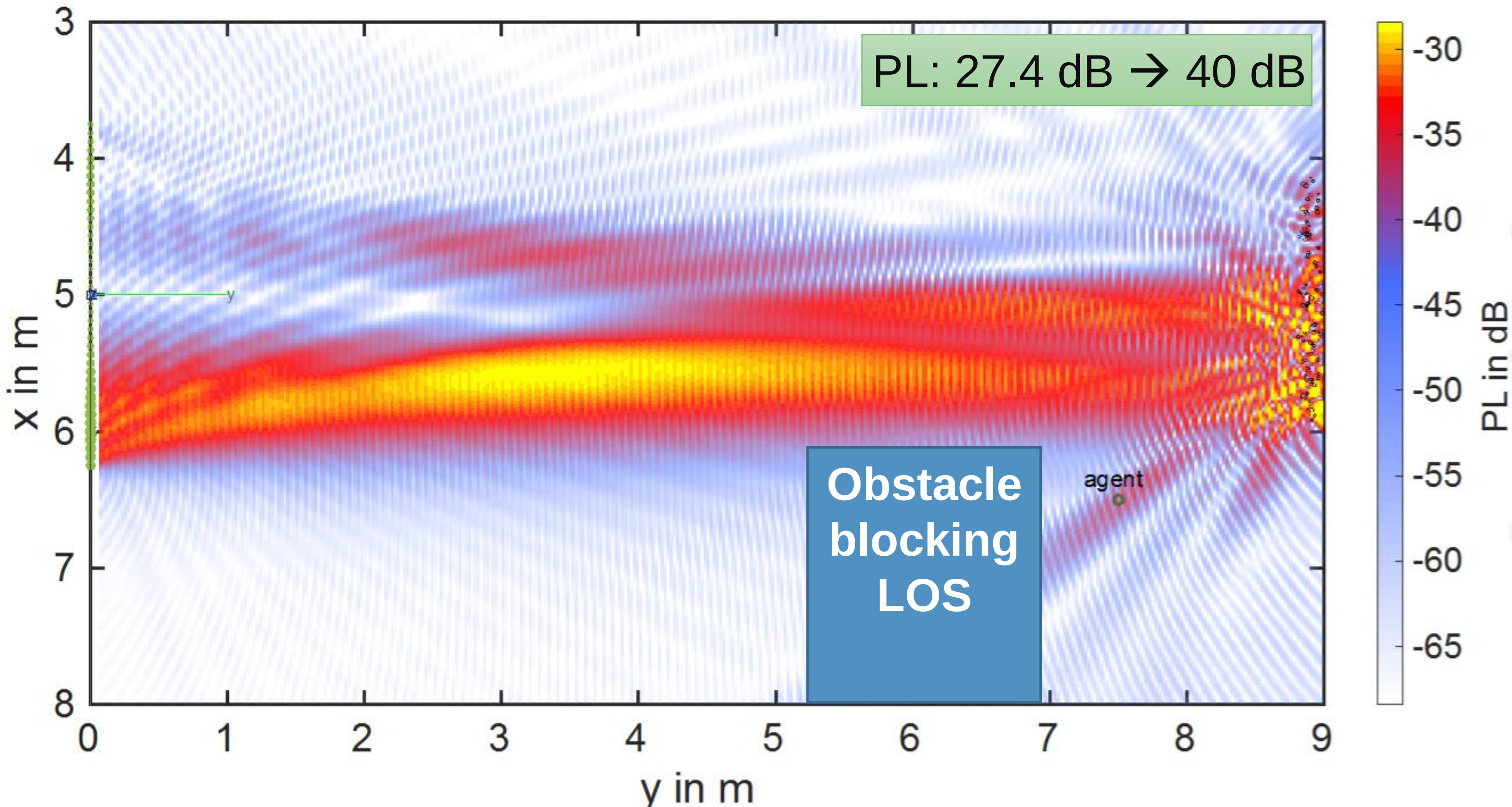

Maximum ratio transmission
assuming perfect channel state

[Illustration: Benjamin Deutschmann]

Scattered component, only

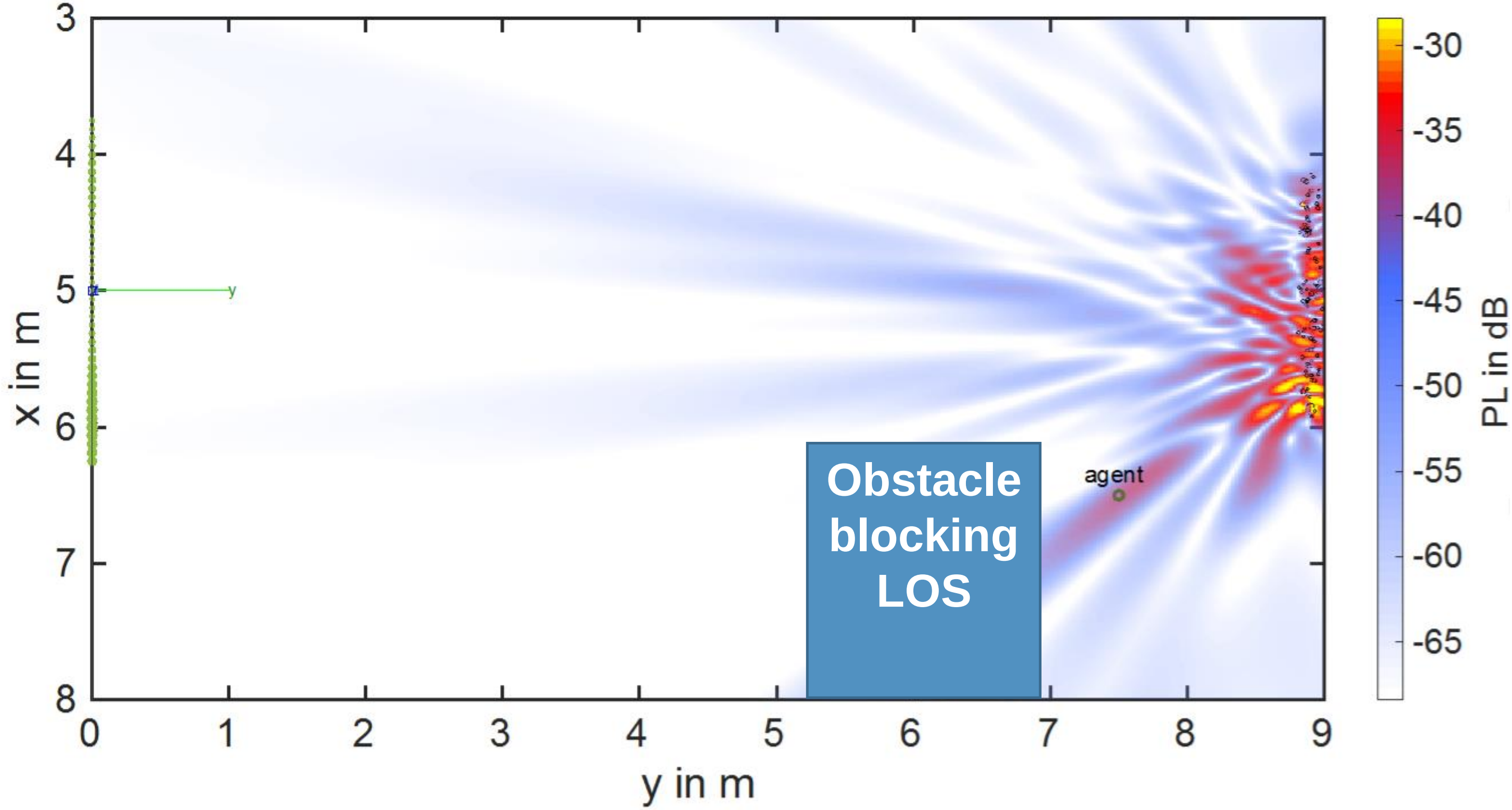

Diffuse reflection from scatter points: **Rayleigh fading**

[Illustration: Benjamin Deutschmann]

Example 3: beam illuminates scatter points

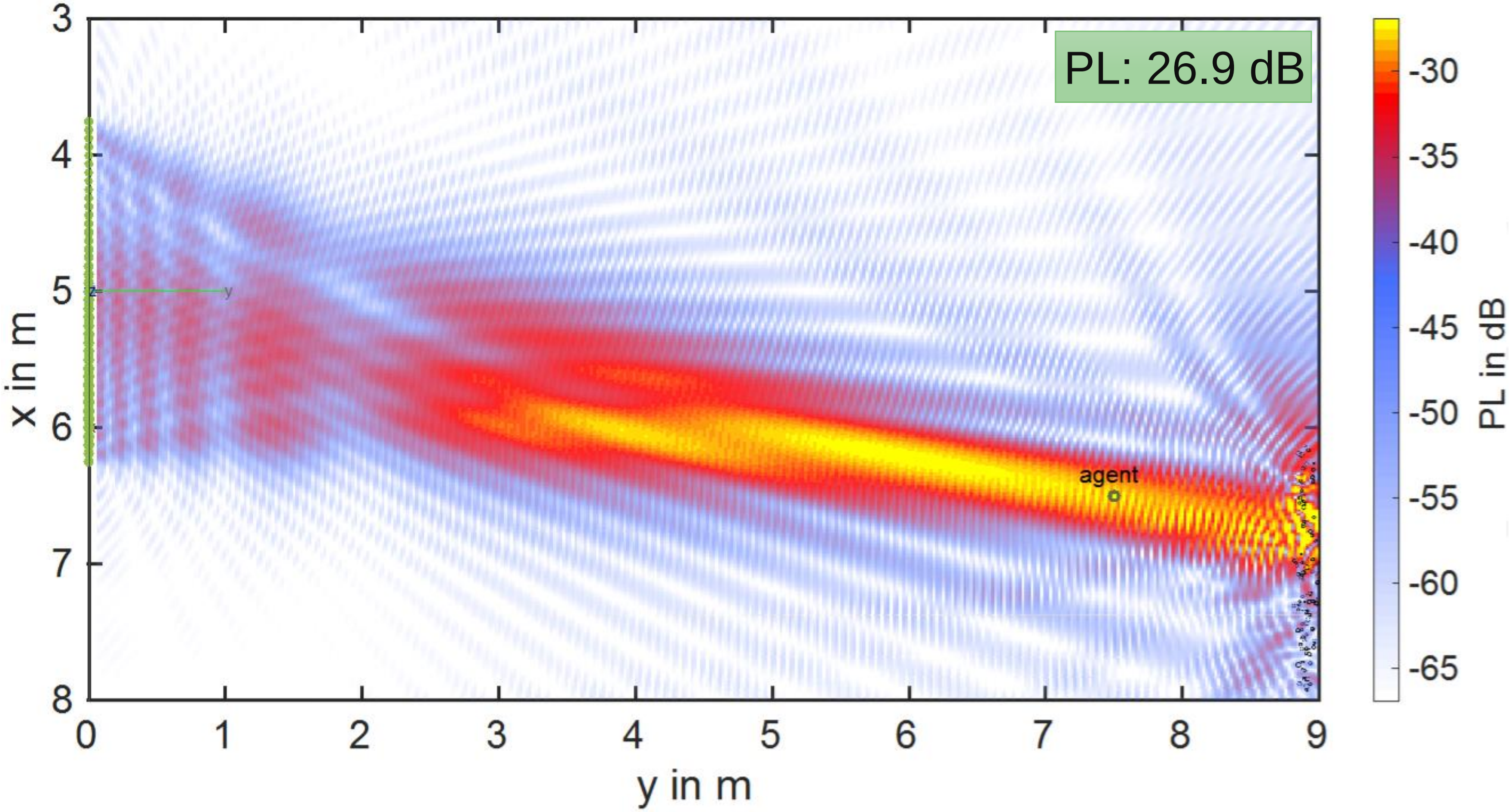

Diffuse reflection from scatter points: **Rayleigh fading**

[Illustration: Benjamin Deutschmann]

Applications

(physically large arrays; distributed mMIMO; RadioWeaves)

- Conclusions from channel modeling:
  - Power **converges** towards user
  - High angle resolution; depth resolution (specular components!)

- Applications:
  - Energy efficient communications; low interference to other users
  - Wireless power transfer (WPT)
  - Positioning and sensing

Conclusions and Outlook

- Distributed massive MIMO (RadioWeaves)
  - A candidate technology for 6G with **unique features**
  - Fundamentally shifted **channel properties**
  - Unprecedented **efficiency** and performance
  - Massive deployment including **batteryless nodes**

- 6G wireless networks will include **sensing** and (robust) positioning
  - **Environment awareness** for long-term predictability
  - Data acquisition for **digital twinning**